Supplementary Inforamation for

Synthesis of 2,7-dioctylbiphenylenodithiophenes for use as organic semiconducting materials in solution-processed organic thin-film transistors

Makoto Watanabe, [a]* Masato Miyashita, [a] Takashi Fukuda [b] and Shinya Oku [a]

[a] *Advanced Materials Research Laboratory, Tosoh Corporation,*
2743-1 Hayakawa, Ayase-shi, Kanagawa, 252-1123 Japan
[b] *Research and Development Planning, Tosoh Corporation,*
2-2-1 Yaesu, Tyuou-ku, Tokyo, 104-8467 Japan

Correspondence should be addressed to M. W. (makoto-watanabe-zr@tosoh.co.jp)

Contents

1. Laser microscope images

The surface morphology of **C8-B1-BPDT** and **C8-B2-BPDT** obtained by drop casting was probed by laser microscope. The sample was prepared by drop casting of 0.2 wt % solution in toluene on a parylene-C.

Fig. S1 Laser microscope images of **C8-B1-BPDT** with PS (left) and **C8-B2-BPDT** (right) (700 × 700 μm).

The laser microscope images obtained by spin coating of three compounds with PS were shown below.

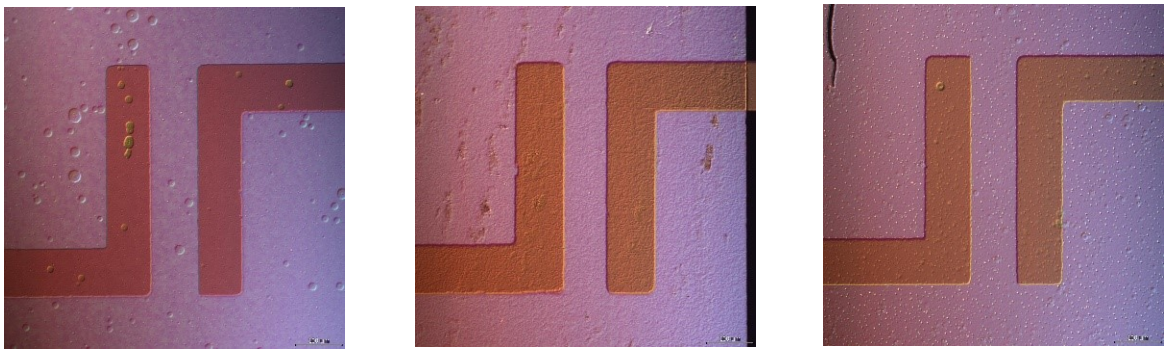

Fig. S2 Laser microscope images of **C8-B1-BPDT** (left), **C8-B2-BPDT** (center) and **C8-L-BPDT** (right) (700 × 700 μm).

2. SEM and AFM images

The surface morphology of the drop-cast films of **C8-B1-BPDT** and **C8-B2-BPDT,** and the vacuum deposition film of **C8-L-BPDT** are shown below.

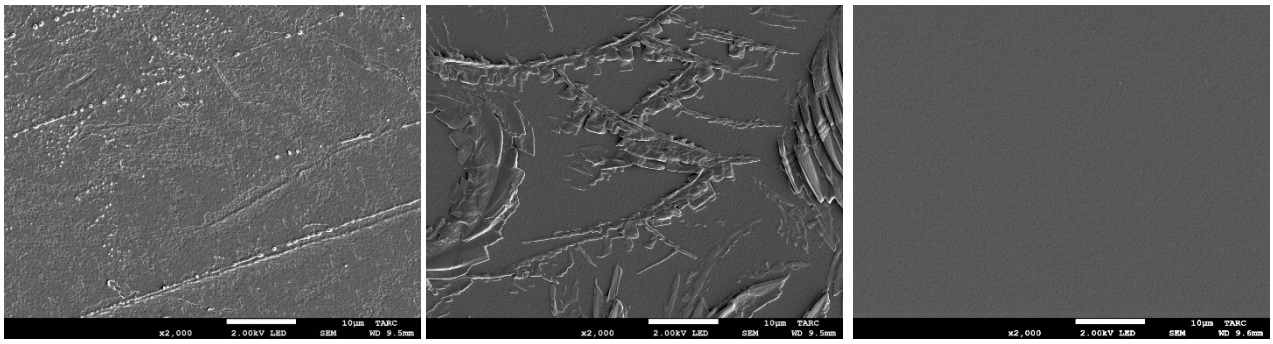

Fig. S3 SEM images (without PS) of **C8-B1-BPDT** (left), **C8-B2-BPDT** (center) and **C8-L-BPDT** (right) (60 × 45 μm).

AFM image of the film of **C8-B1-BPDT** (average surface roughness, *R*a = 11 nm) is so rough that grains cannot be confirmed. It also has deep cavities in the order of tens of nanometers. This could be related to the fact that the interface between the dielectric and the organic semiconductor layer is critical. The films of **C8-B2-BPDT** (*R*a = 4.3 nm) and **C8-L-BPDT** (*R*a = 3.7 nm) have relatively smaller roughness and the irregular fine grains.

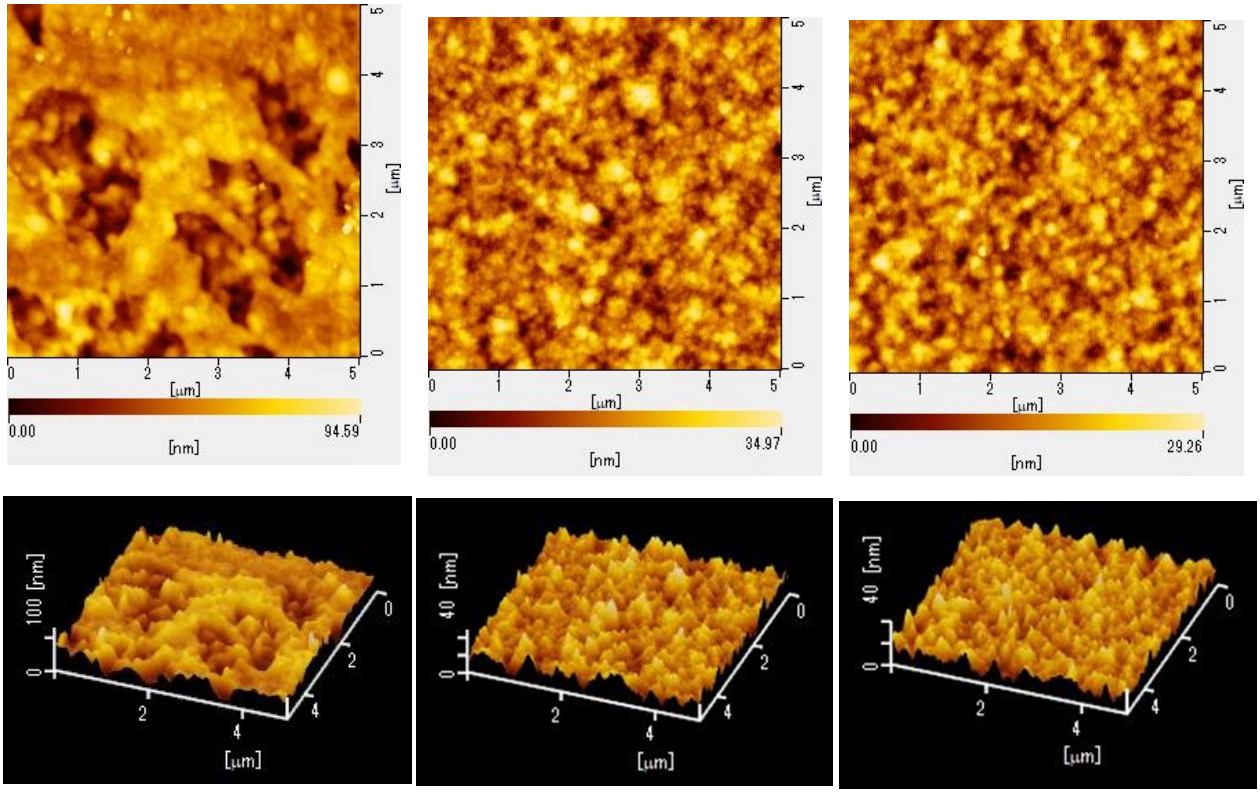

Fig. S4 AFM images (without PS) of **C8-B1-BPDT** (left), **C8-B2-BPDT** (center) and **C8-L-BPDT** (right) (5 × 5 µm).

The surface morphology of the drop-cast films of **C8-B1-BPDT** including PS are shown below. AFM image the film of **C8-B1-BPDT** including PS (*R*a = 12 nm) is also rough and has deep ditches in the order of tens of nanometers.

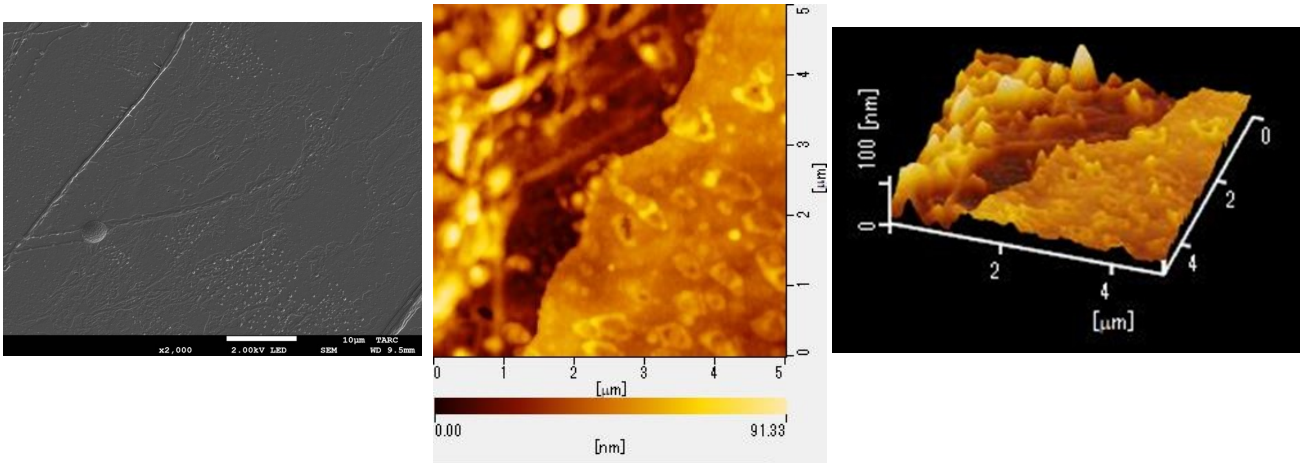

Fig. S5 SEM (left, 60 × 45 µm) and AFM (center and right, 5 × 5 µm) images of a drop-cast thin film of **C8-B1-BPDT** with PS.

3. UV-vis spectra of **C8-B2-BPDT** and **C8-L-BPDT** in dichloromethane

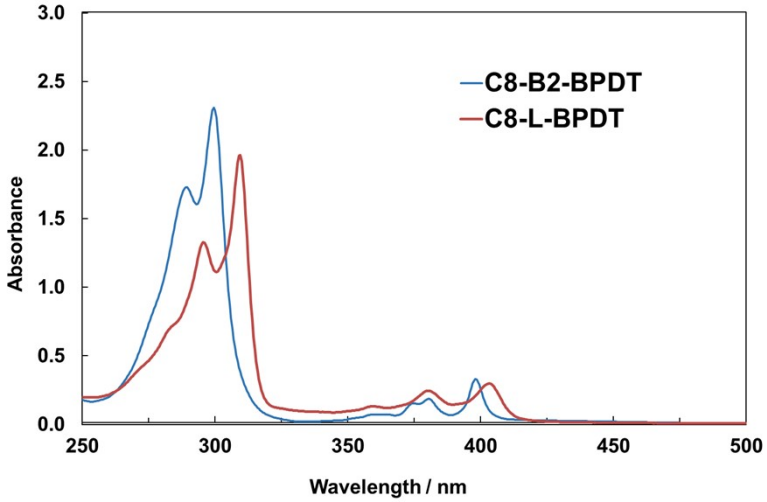

Fig. S6 UV-Vis spectra of of **C8-B2-BPDT** and **C8-L-BPDT** in dichloromethane solution.

4. Photoelectron spectroscopy in air

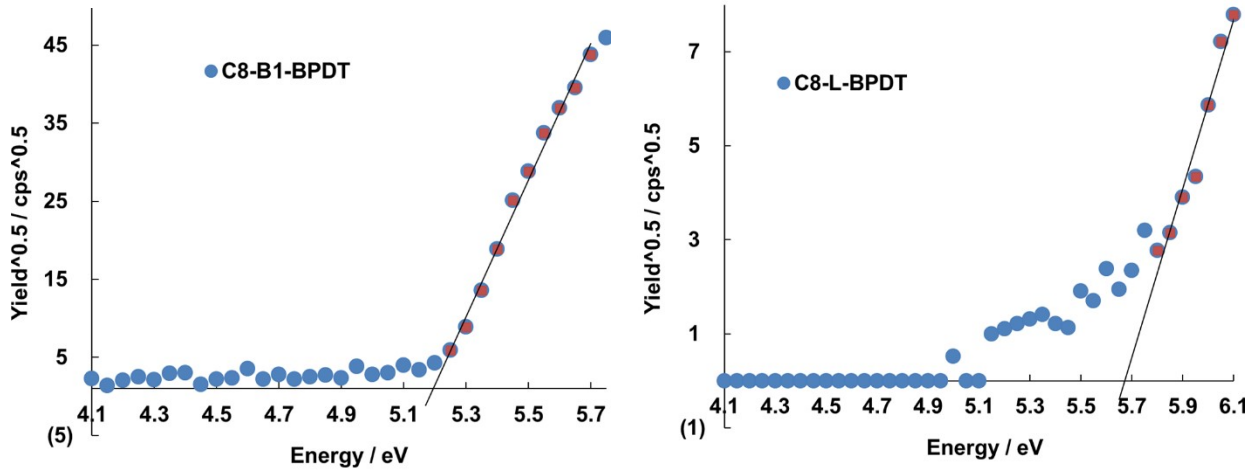

Fig. S7 Photoelectron spectra of **C8-B1-BPDT** thin films prepared by drop casting and **C8-L-BPDT** prepared by vacuum deposition.

5. DSC of **C8-B2-BPDT** and **C8-L-BPDT**

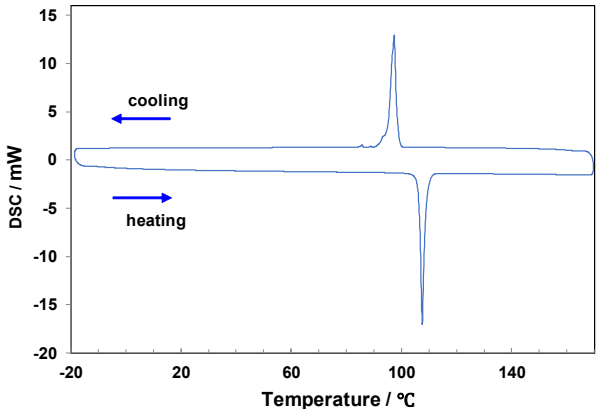

Fig. S8.1 DSC curves of **C8-B2-BPDT**.

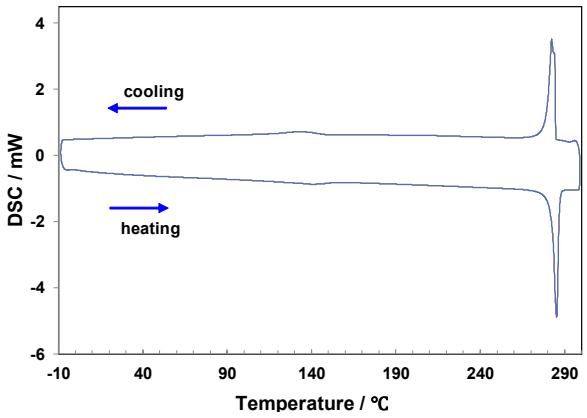

Fig. S8.2 DSC curves of **C8-L-BPDT**.

6. Out of plane X-ray diffraction

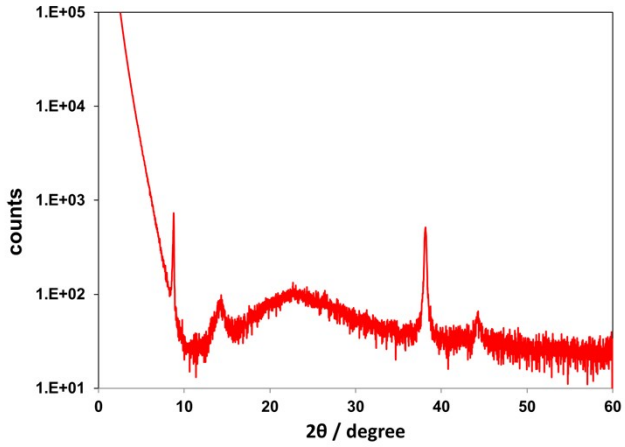

Fig. S9.1 XRD of drop-cast thin film of **C8-B2-BPDT**.

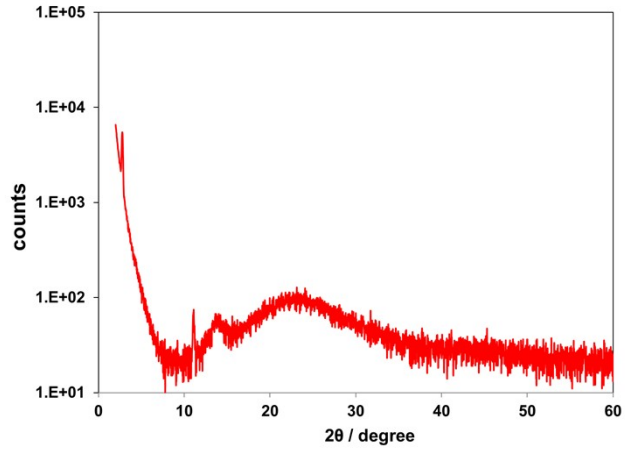

Fig. S9.2 XRD of vacuum deposited thin film of **C8-L-BPDT**.

7. Crystallographic parameters

6.1 Crystallographic parameters

Table S1 Crystallographic parameters

Compounds	**C8-B1-BPDT**	**C8-B2-BPDT**
Chemical formula	$C_{32}H_{40}S_2$	$C_{32}H_{40}S_2$
D_{calc} / g cm^{-3}	1.200	1.221
Formula weight	488.76	488.76
Crystal system	monoclinic	triclinic
Space group	*I*2/*a*	*P*-1
a / Å	10.9056 (4)	5.72410 (10)
b / Å	4.7333 (2)	11.0388 (2)
c / Å	52.478 (2)	11.8971 (3)
α / deg	90	116.814 (2)
β / deg	93.015 (3)	95.590 (2)
γ / deg	90	92.275 (2)
V / Å^3	2705.13 (18)	664.76 (3)
Z value	4	1
T / K	100	100
Wavelength / Å	1.54184	1.54184
Radiation type	CuK_α	CuK_α
Measured reflection	9144	10389
Goodness of fit imdicator	1.056	1.028
R (I > 2(I))	0.0572	0.0346
wR2 (all data)	0.1581	0.0919

6.2 Crystal structure of **C8-B2-BPDT**

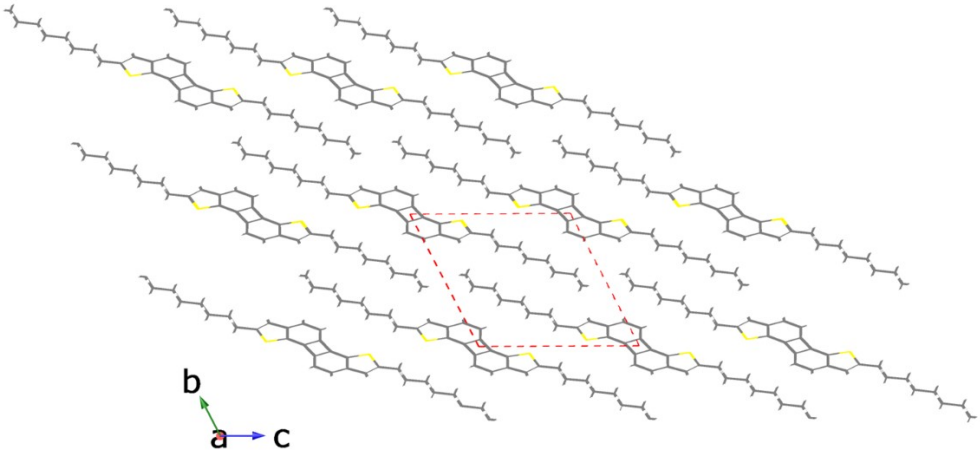

Fig. S10 Crystal structure of **C8-B2-BPDT**.

8. OTFT devices

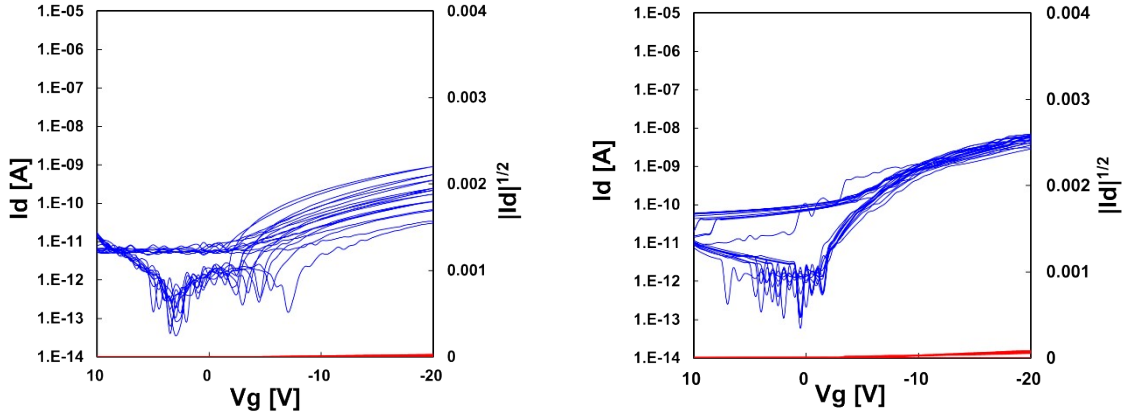

Fig. S11 Transfer characteristics (V_{DS} = −20 V) of **C8-B2-BPDT** thin films prepared by drop casting (left) and **C8-L-BPDT** prepared by vacuum deposition.

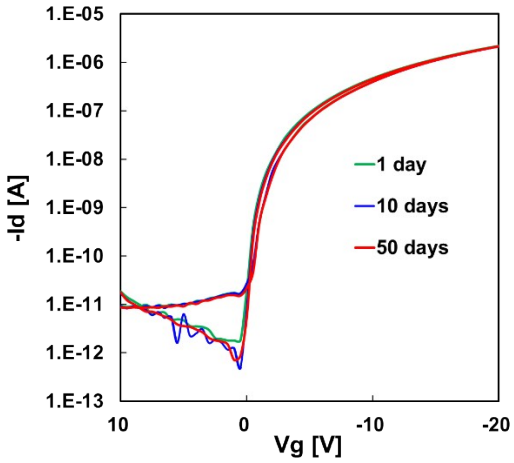

Fig. S12 Transfer characteristics (V_{DS} = −20 V) of OTFTs with drop-cast **C8-B1-BPDT** layers including PS after storage 1, 10 and 50 days under ambient conditions. The transfer characteristics after 50 days are virtually not changed.

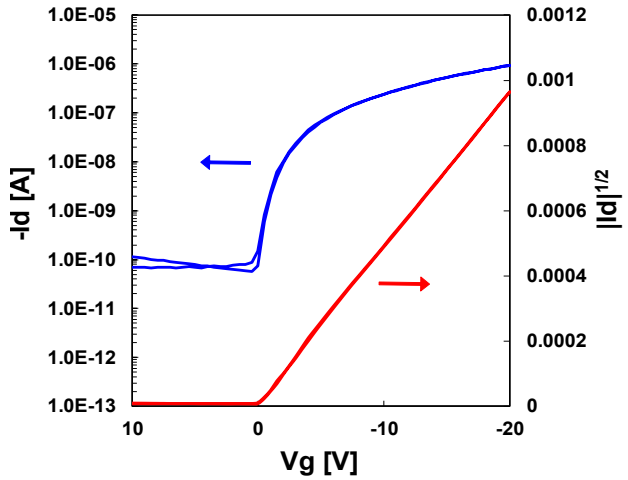

Fig. S13 Transfer characteristics (V_{DS} = −20 V) of OTFTs with drop-cast **C8-B1-BPDT** layers not including PS.

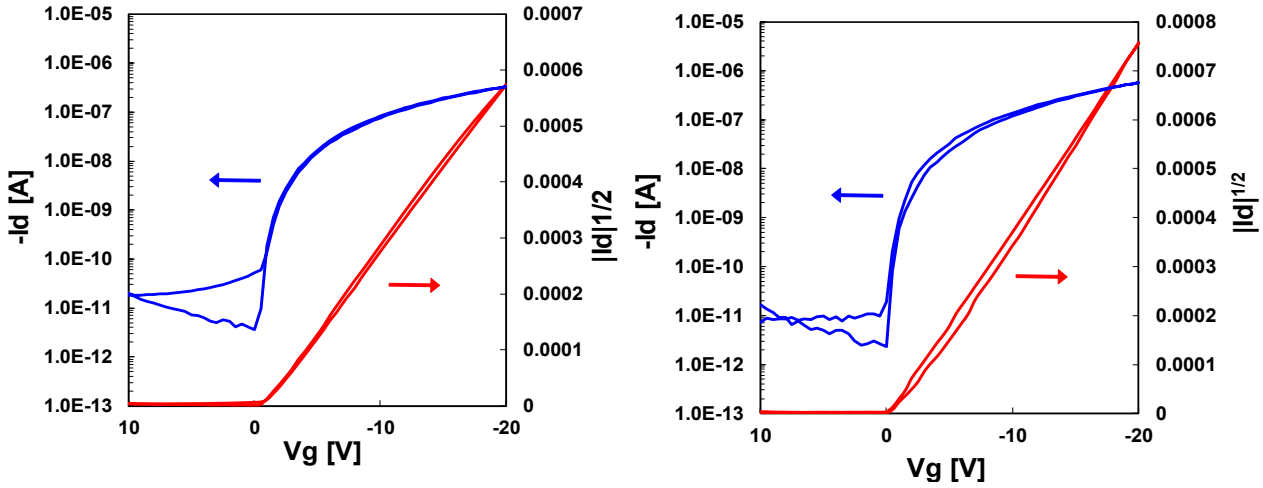

Fig. S14 Transfer characteristics (V_{DS} = −20 V) of OTFTs with spin coating **C8-B1-BPDT** layers not including PS (left) and including PS (right).

9. Interface trap density

Table S2. The interface trap density (*D*it) values

Semiconductor layer	Deposition method	*SS* [V dec^{-1}]	*D*it [eV^{-1} cm^{-2}]
C8-B1-BPDT	drop casting	0.56	3.3×10^{11}
C8-B1-BPDT + PS	drop casting	0.29	1.2×10^{11}
C8-B1-BPDT	spin coating	0.39	2.2×10^{11}
C8-B1-BPDT + PS	spin coating	0.33	1.7×10^{11}

10. NMR spectra

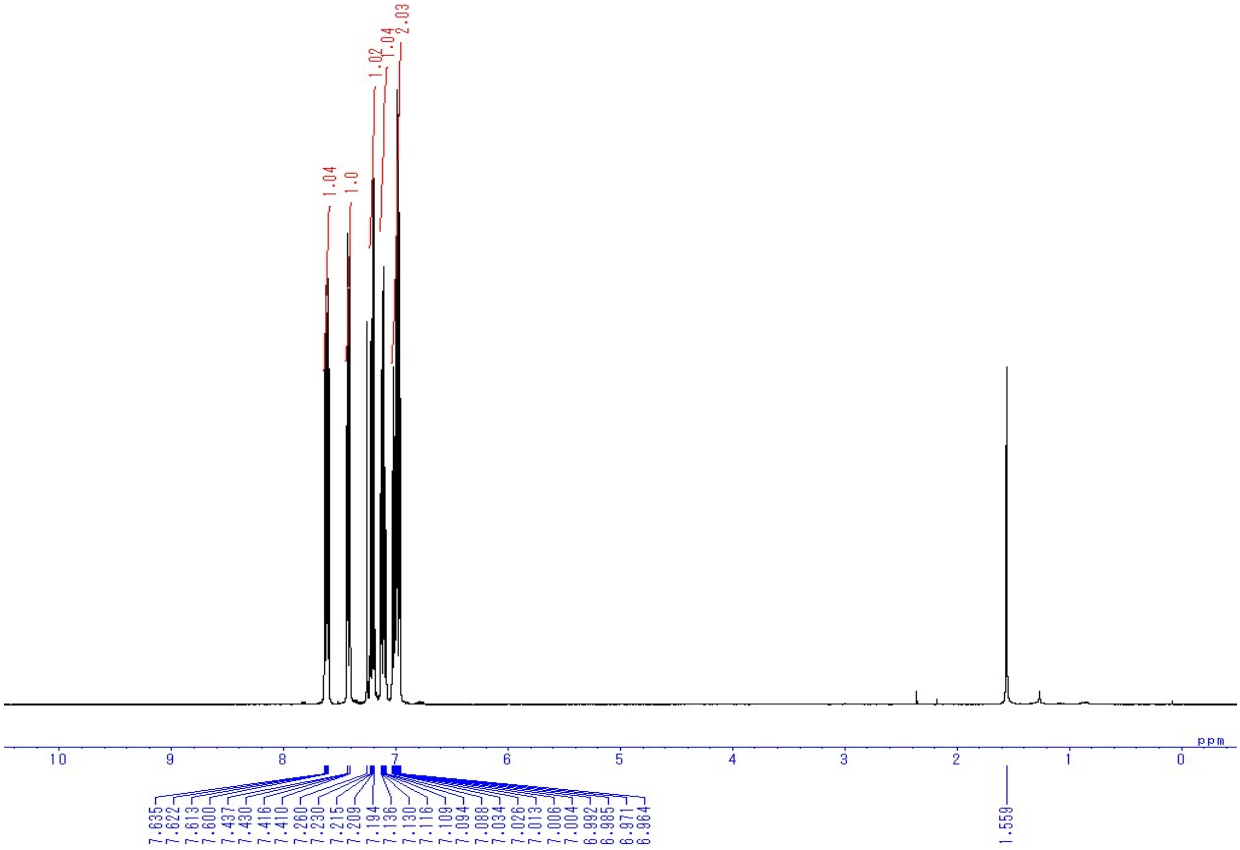

Fig. S15.1 ^{1}H NMR spectrum of **3**

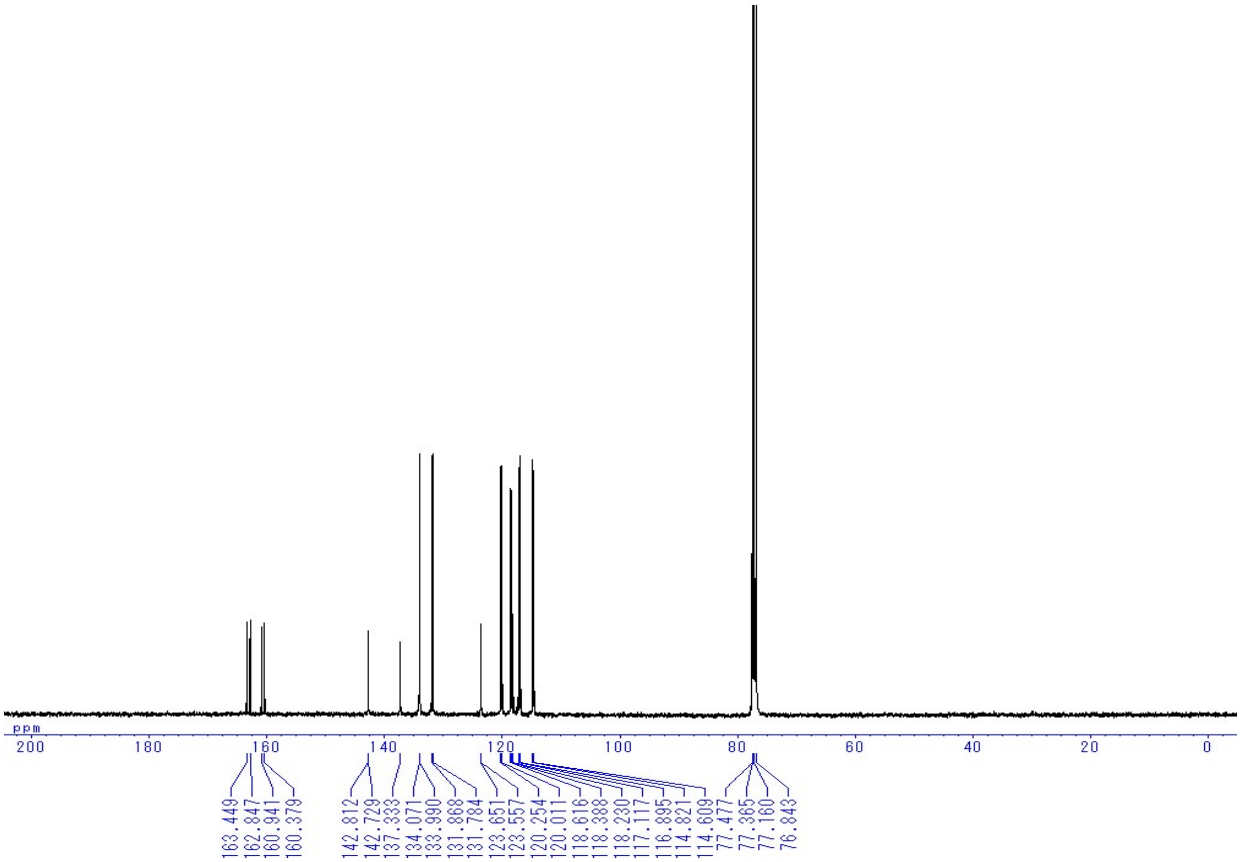

Fig. S15.2 ^{13}C NMR spectrum of **3**

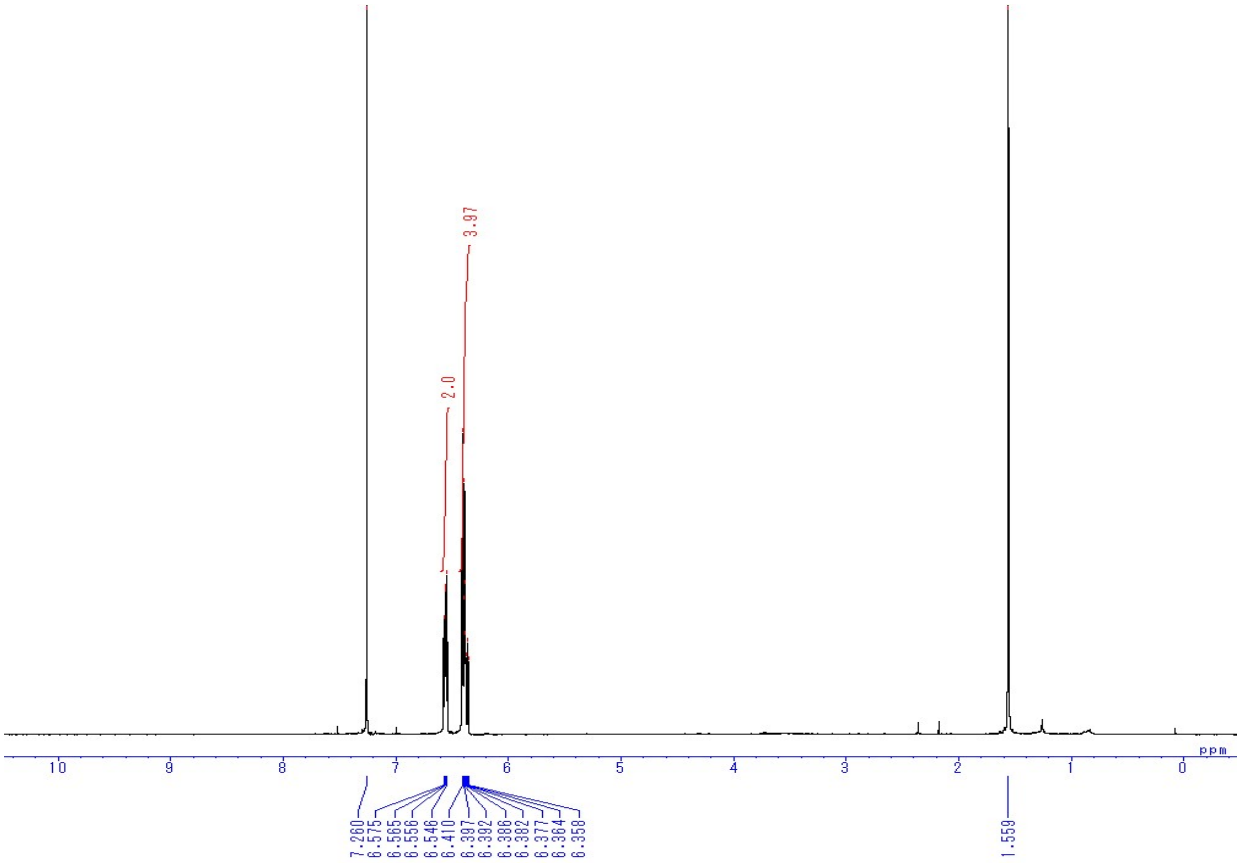

Fig. S15.3 ^{1}H NMR spectrum of **4**

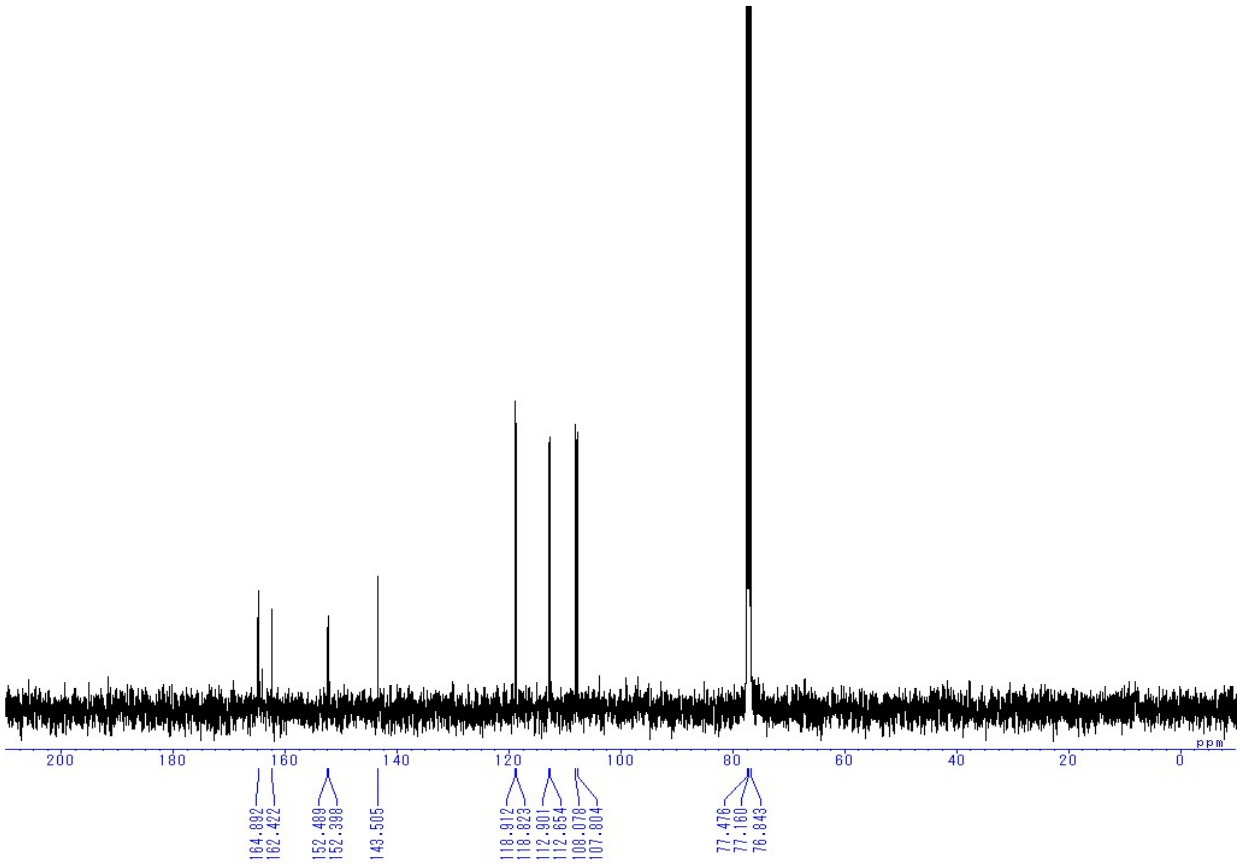

Fig. S15.4 ^{13}C NMR spectrum of **4**

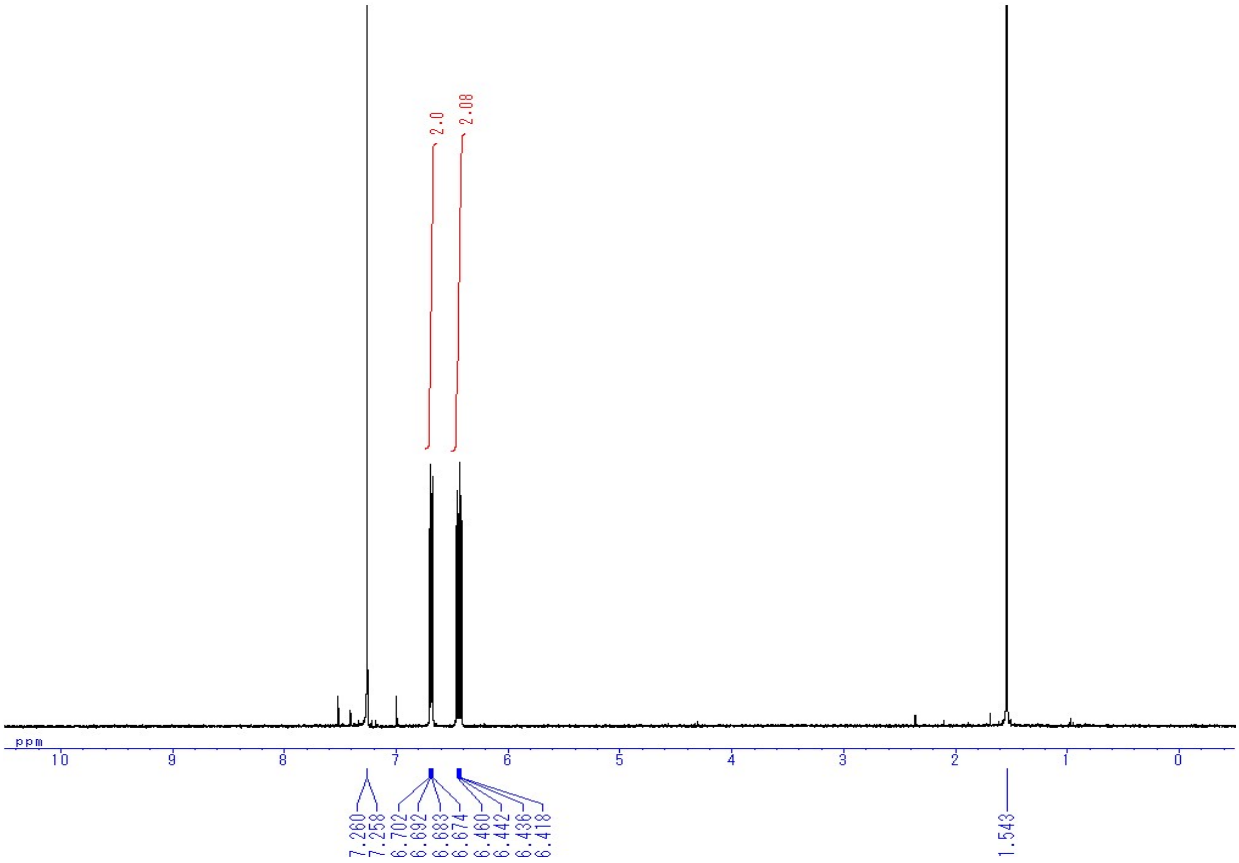

Fig. S15.5 ^{1}H NMR spectrum of **5**

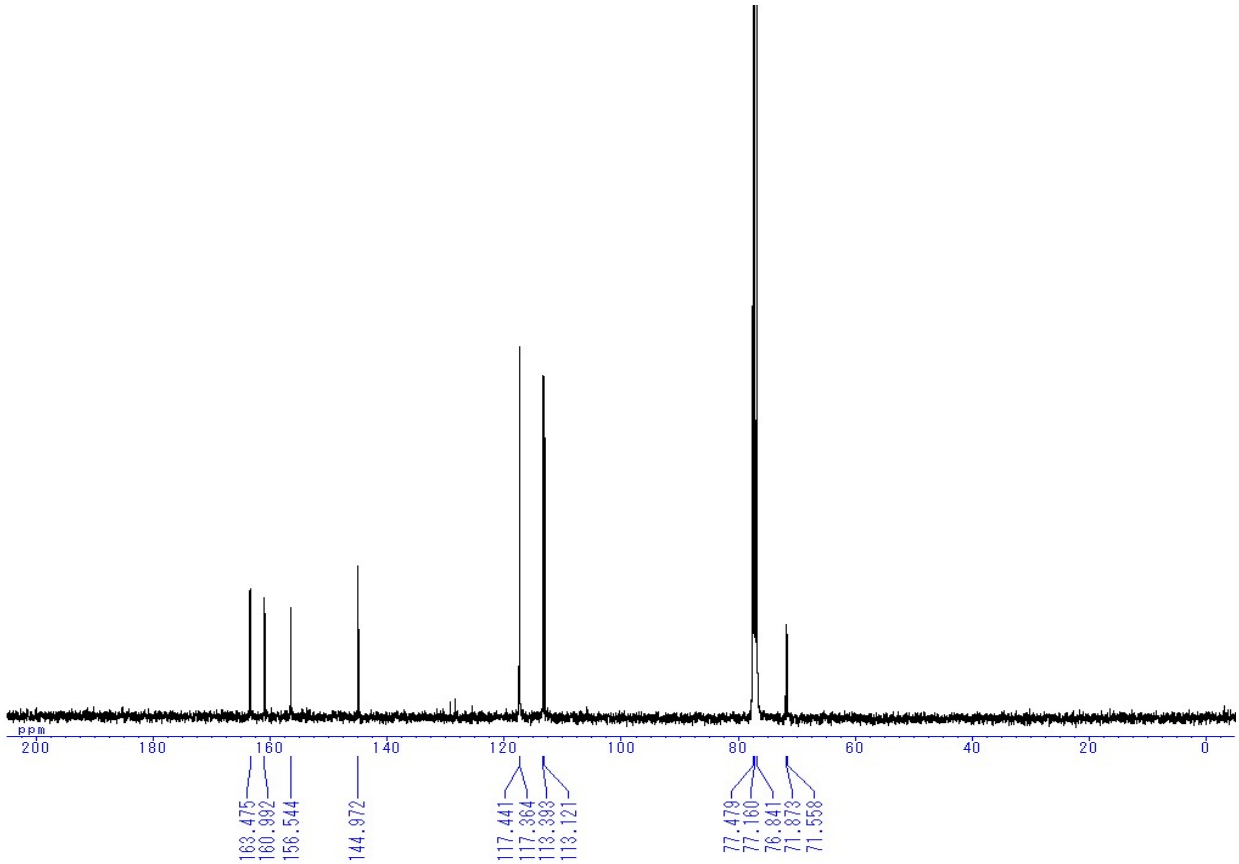

Fig. S15.6 ^{13}C NMR spectrum of **5**

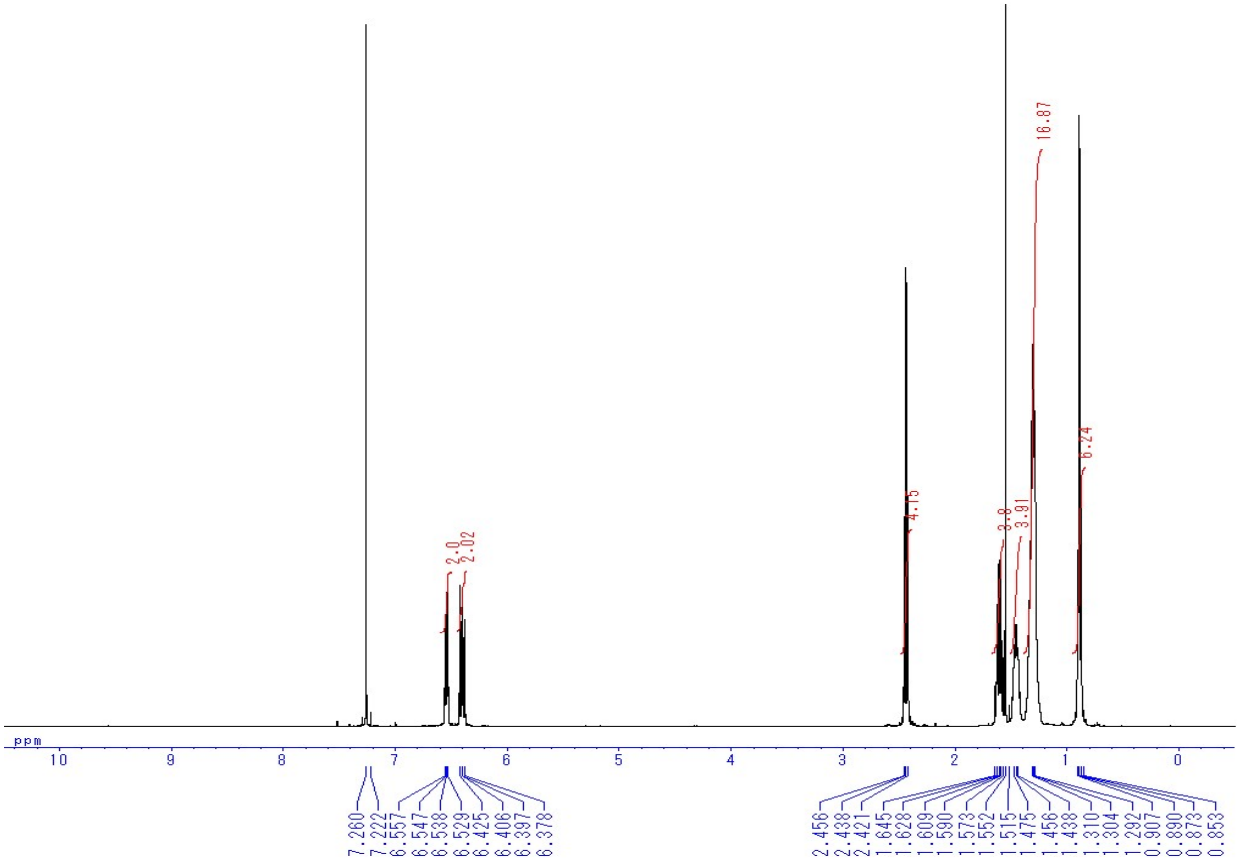

Fig. S15.7 ^{1}H NMR spectrum of **7**

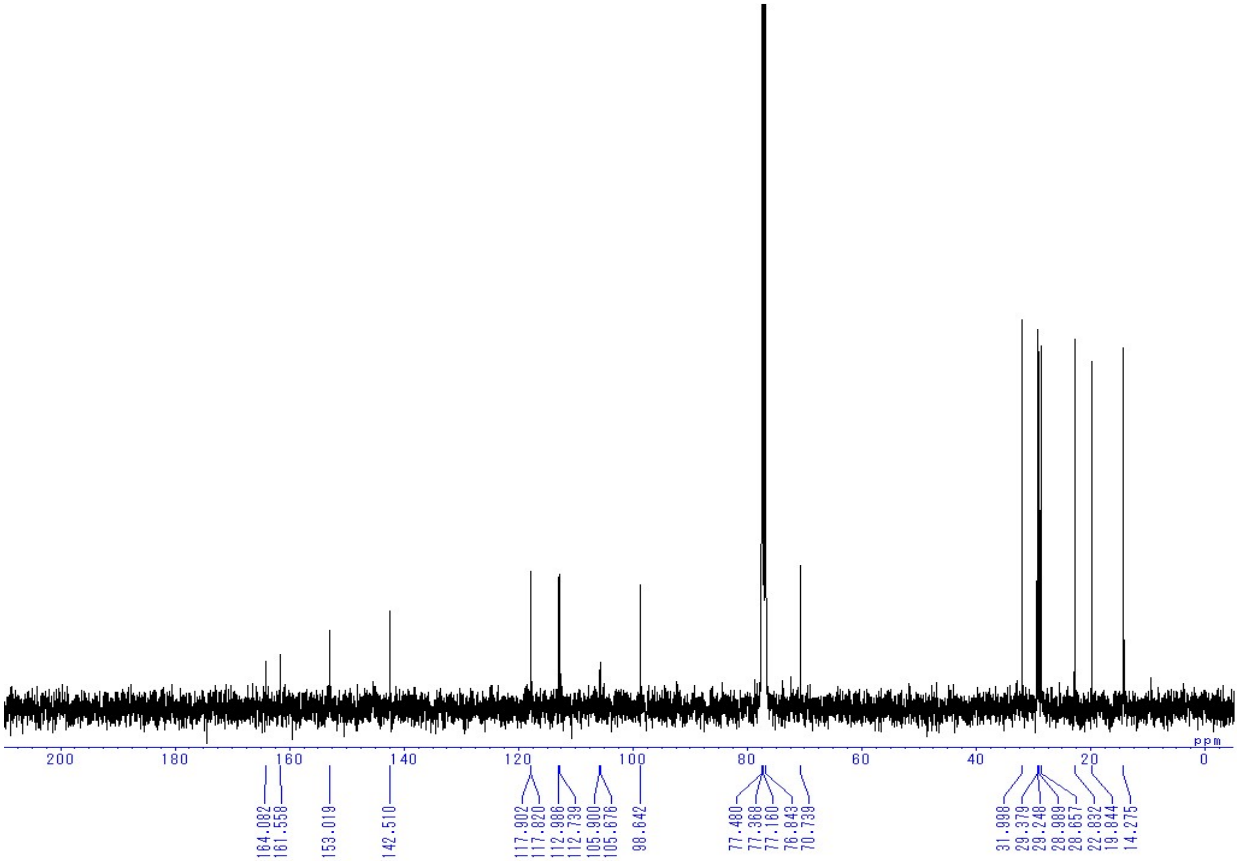

Fig. S15.8 ^{13}C NMR spectrum of **7**

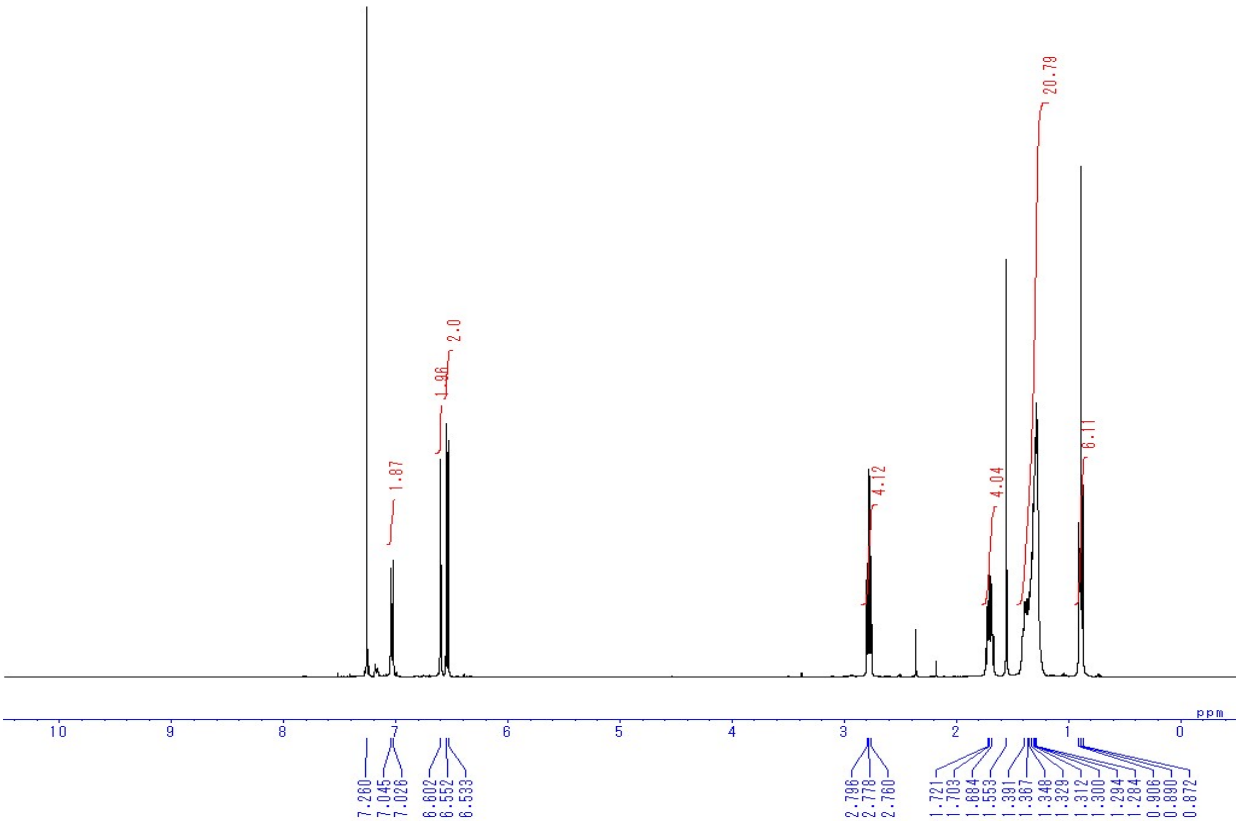

Fig. S15.9 ^{1}H NMR spectrum of **C8-B1-BPDT**

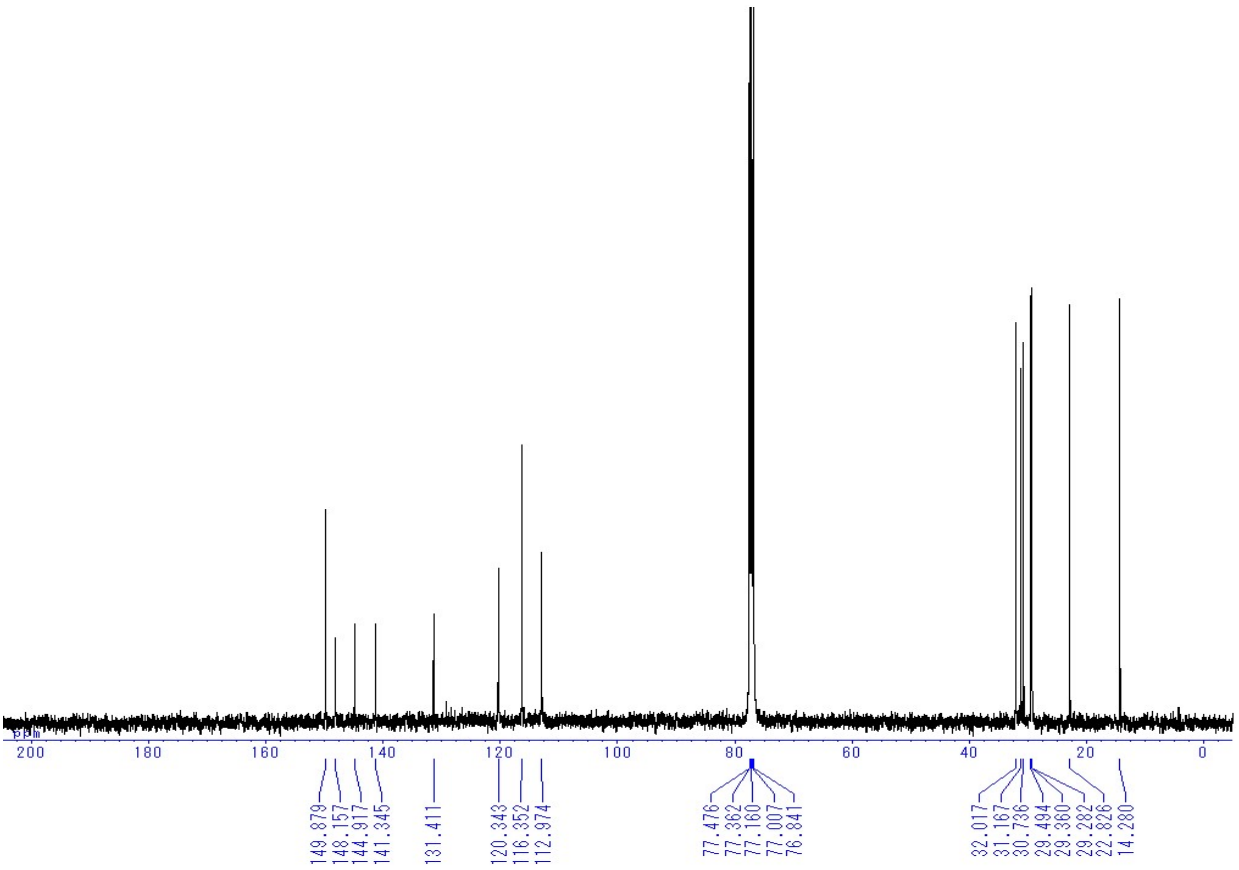

Fig. S15.10 ^{13}C NMR spectrum of **C8-B1-BPDT**

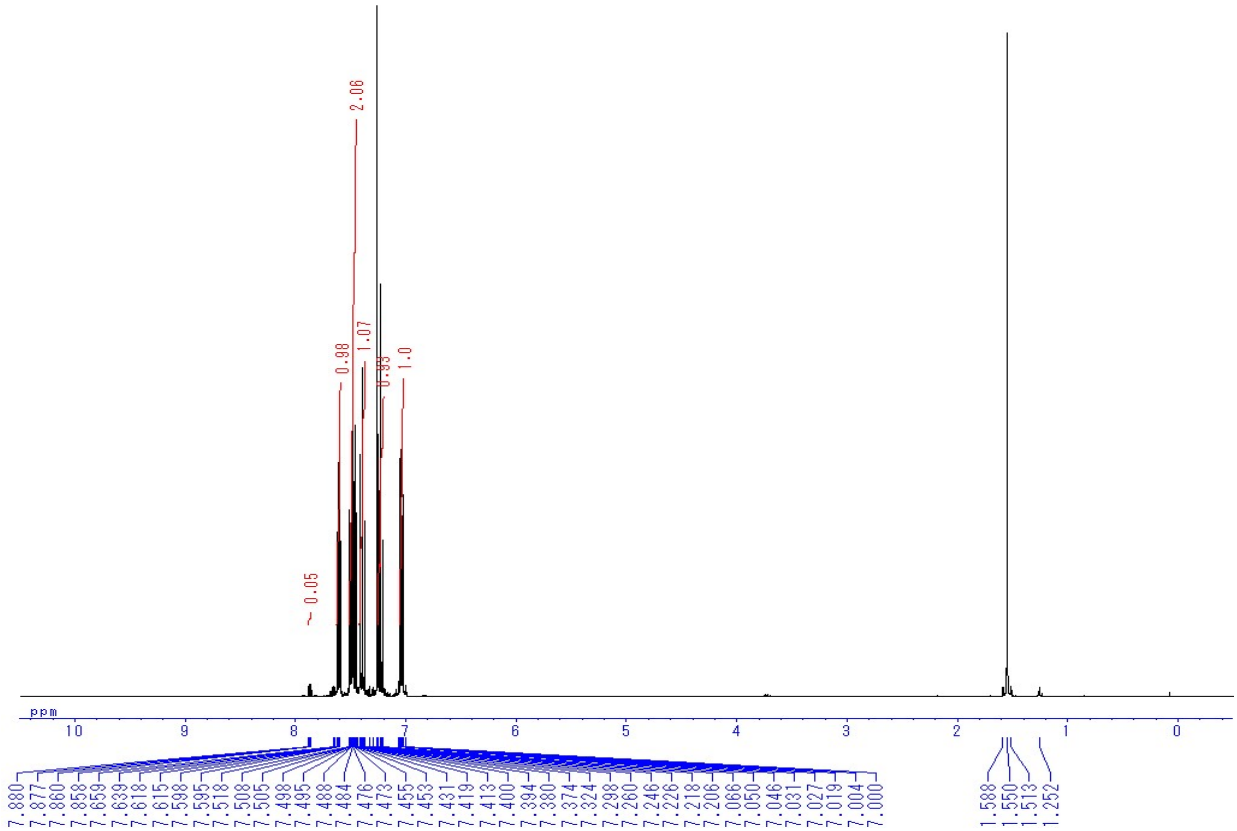

Fig. S15.11 ^{1}H NMR spectrum of **9**

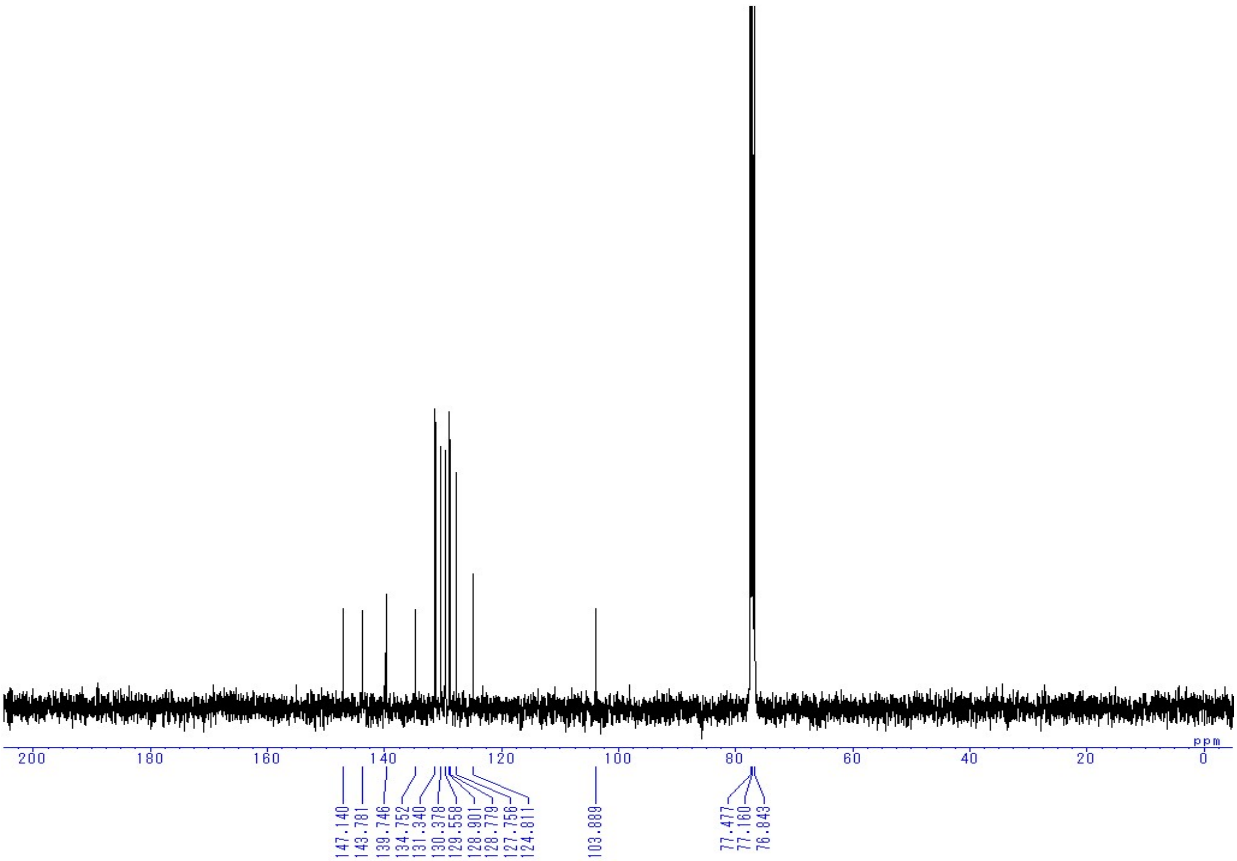

Fig. S15.12 ^{13}C NMR spectrum of **9**

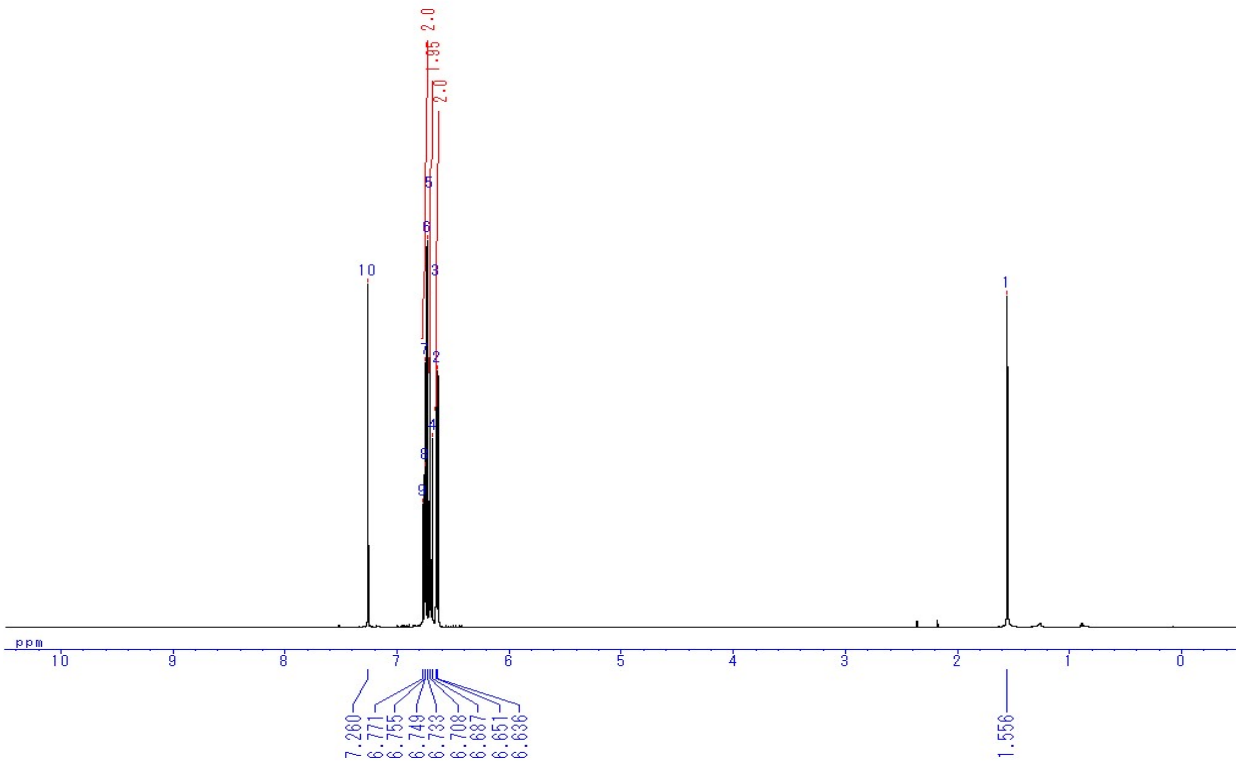

Fig. S15.13 ^{1}H NMR spectrum of **10**

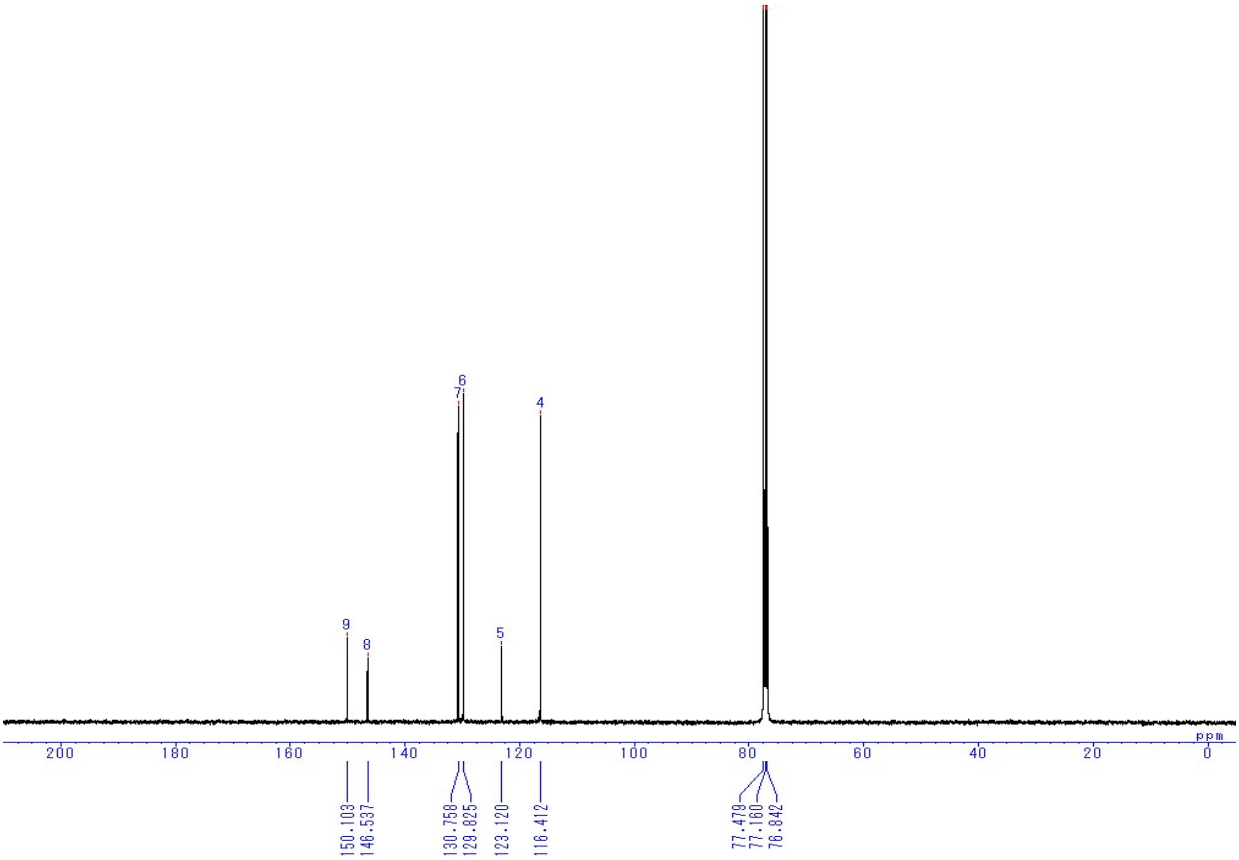

Fig. S15.14 ^{13}C NMR spectrum of **10**

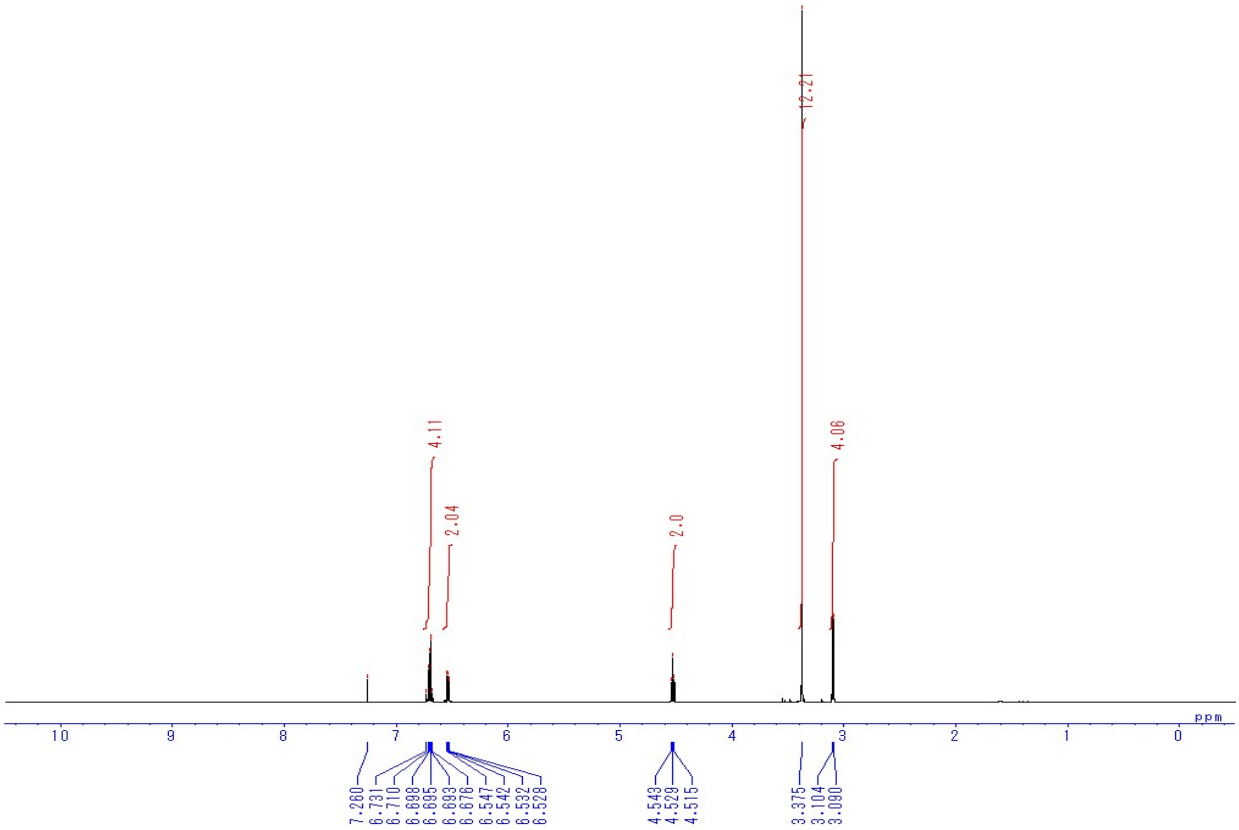

Fig. S15.15 ^{1}H NMR spectrum of **11**

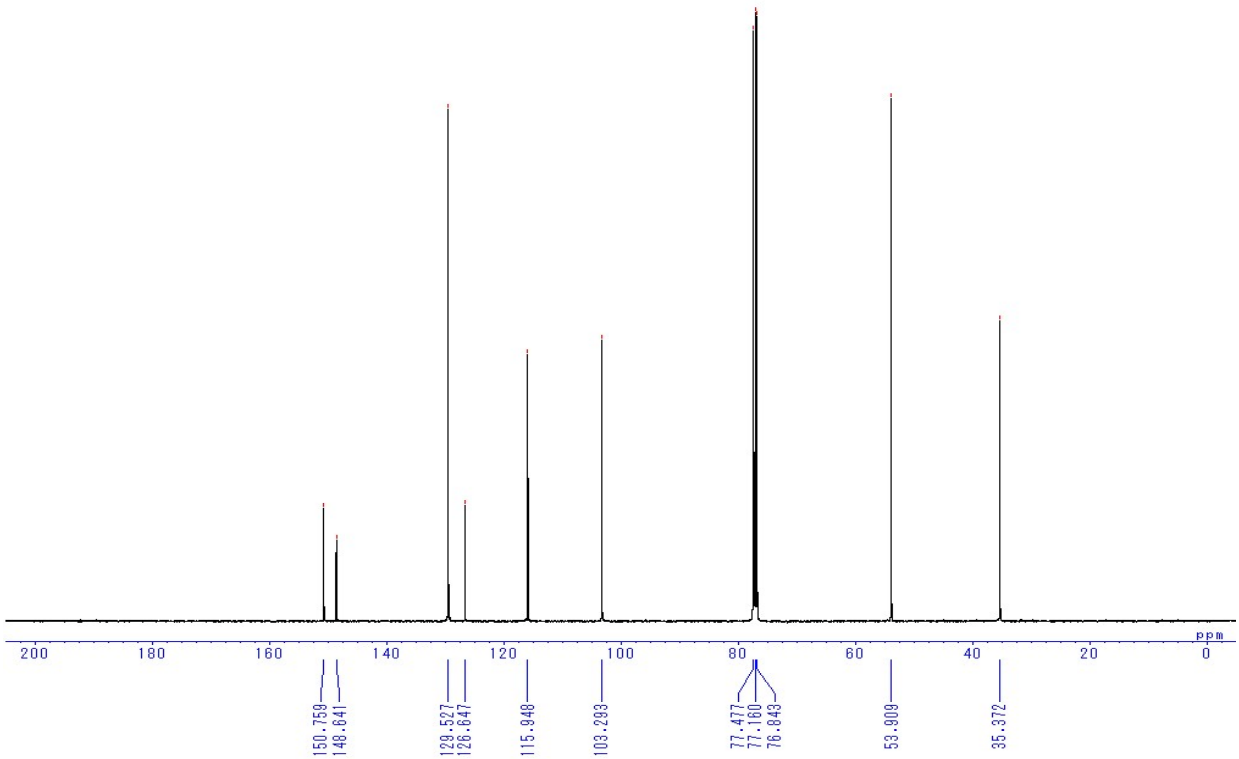

Fig. S15.16 ^{13}C NMR spectrum of **11**

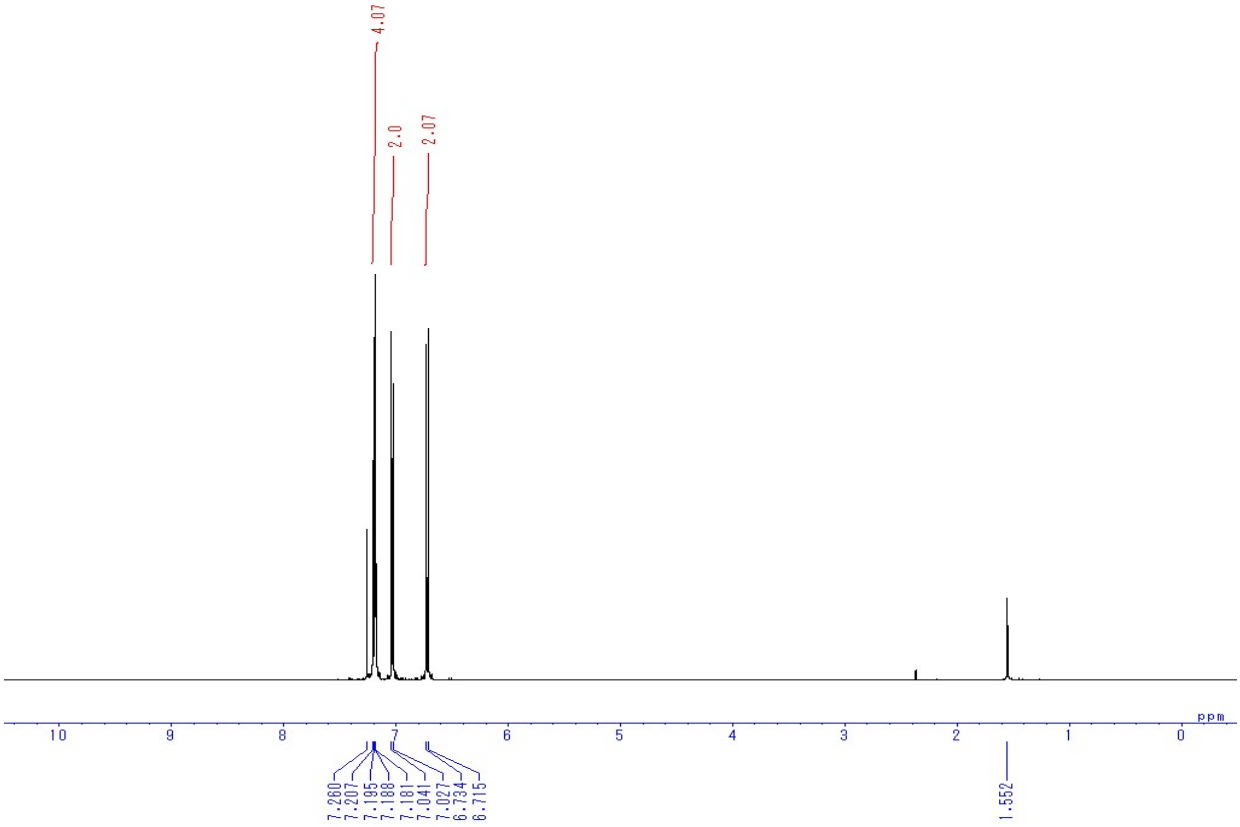

Fig. S15.17 ^{1}H NMR spectrum of **12**

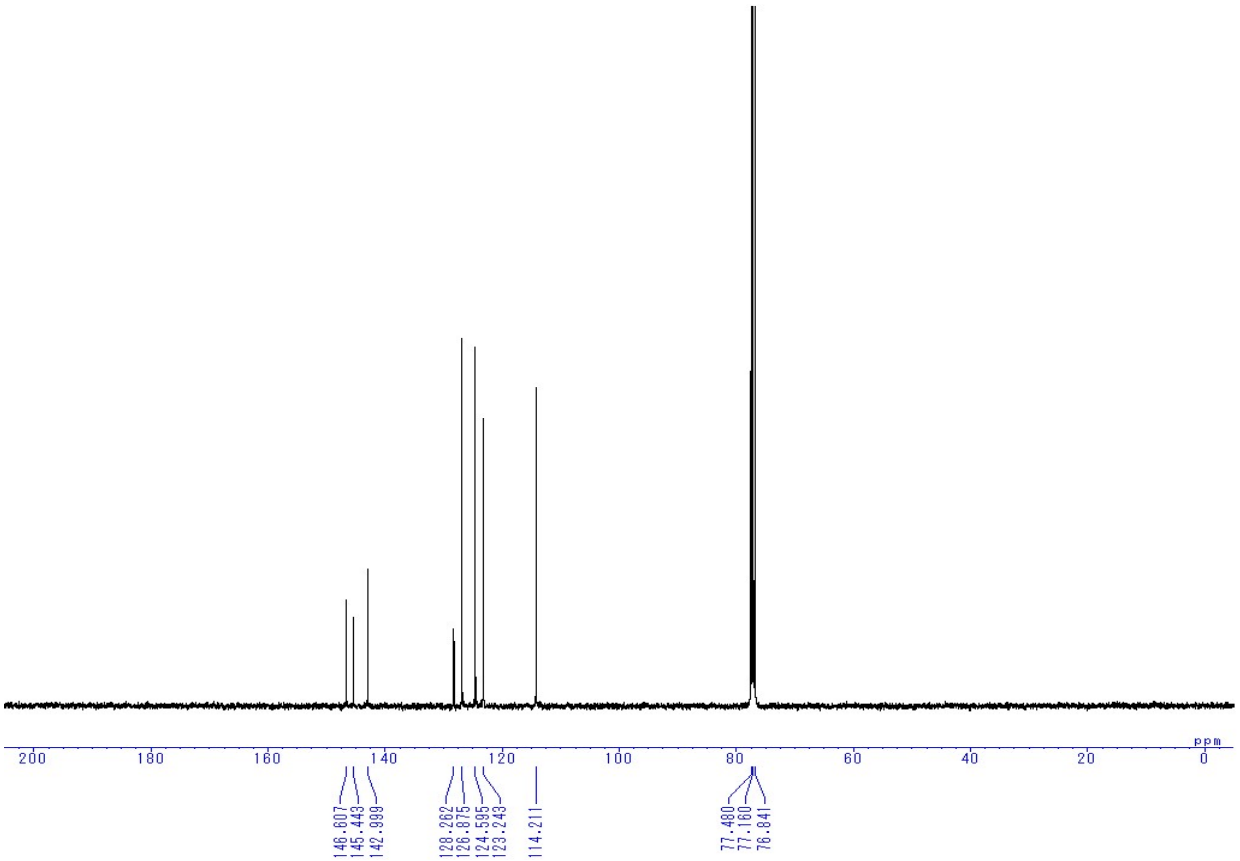

Fig. S15.18 ^{13}C NMR spectrum of **12**

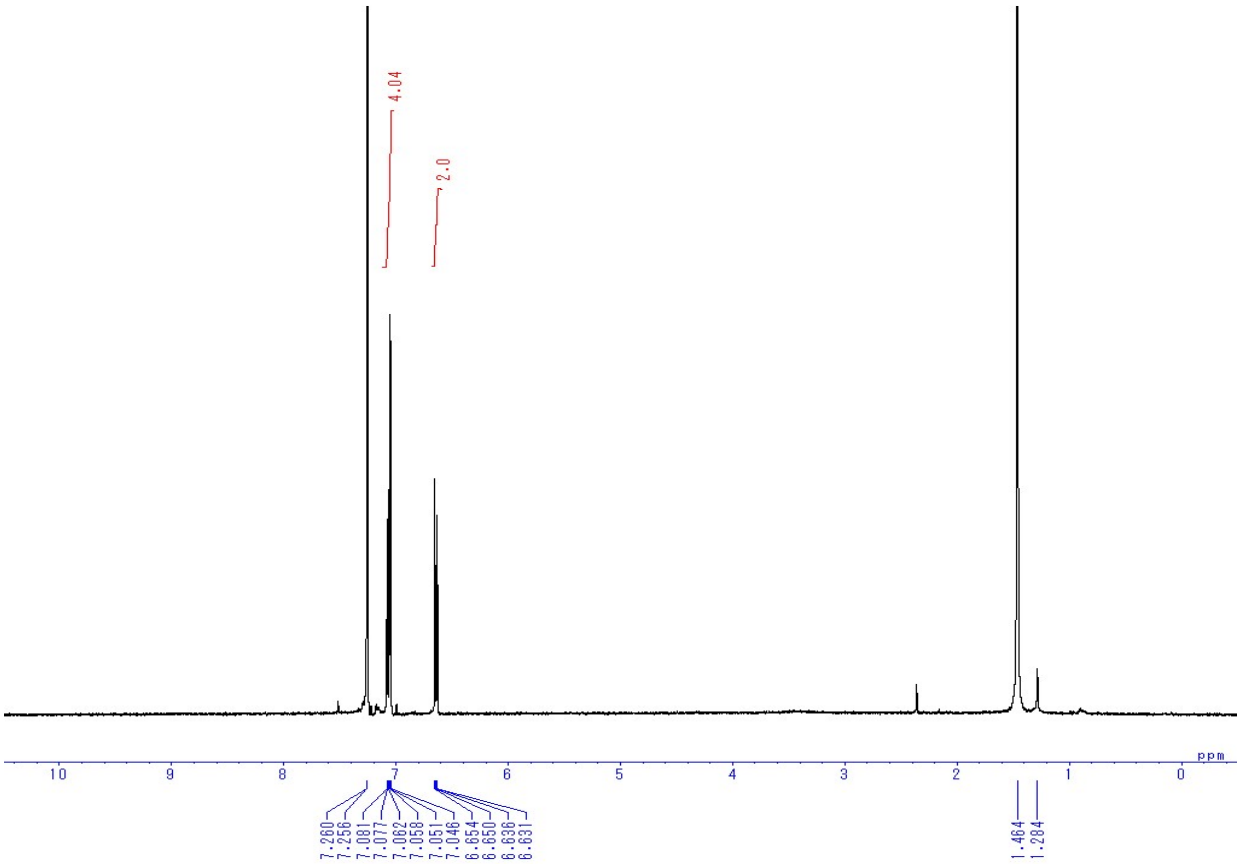

Fig. S15.19 ^{1}H NMR spectrum of **13**

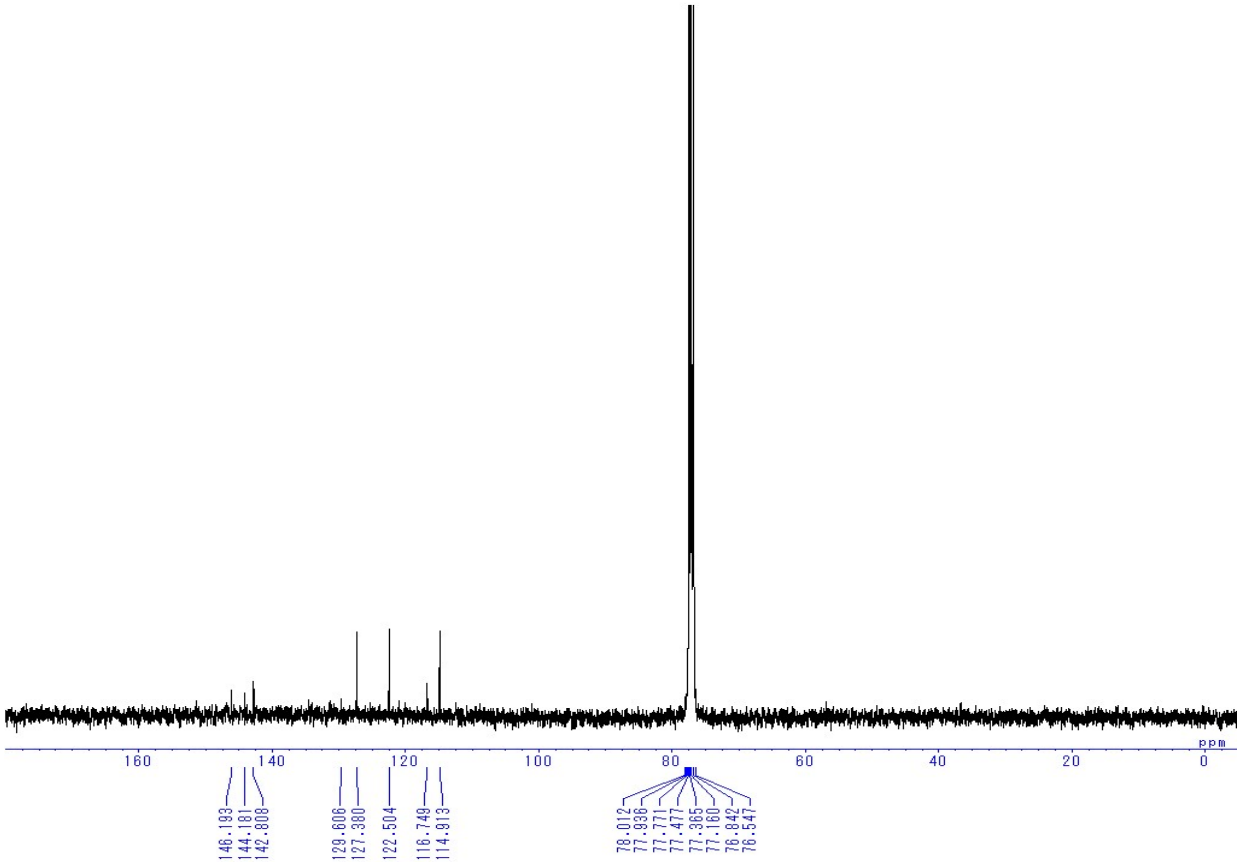

Fig. S15.20 ^{13}C NMR spectrum of **13**

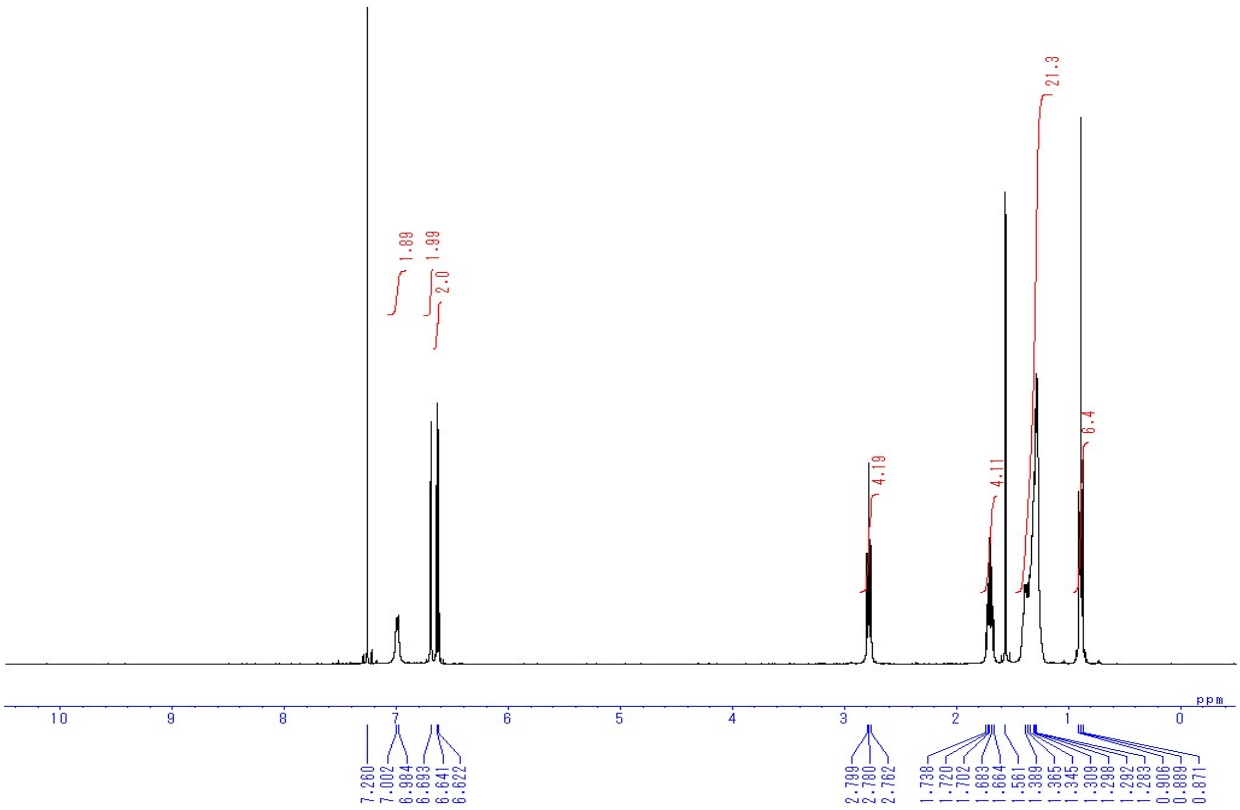

Fig. S15.21 ^{1}H NMR spectrum of **C8-B2-BPDT**

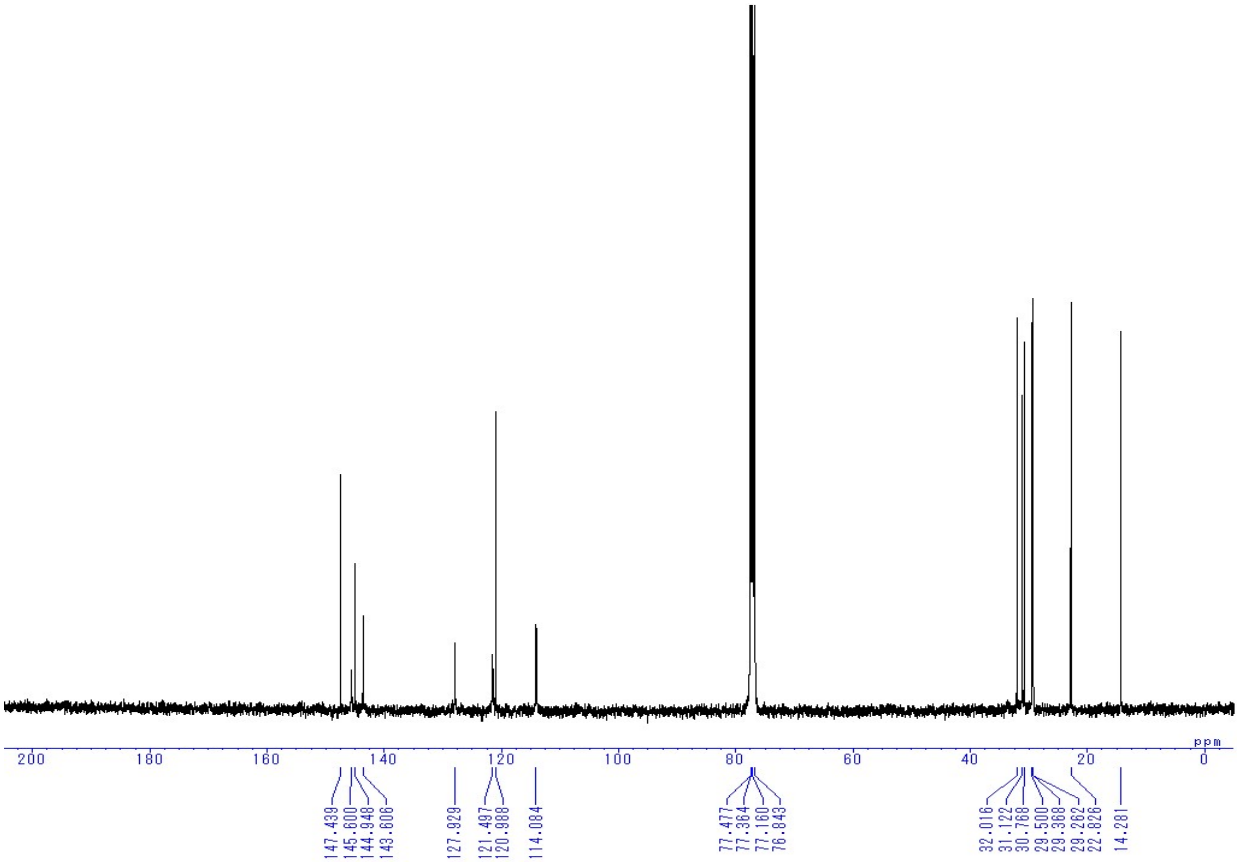

Fig. S15.22 ^{13}C NMR spectrum of **C8-B2-BPDT**

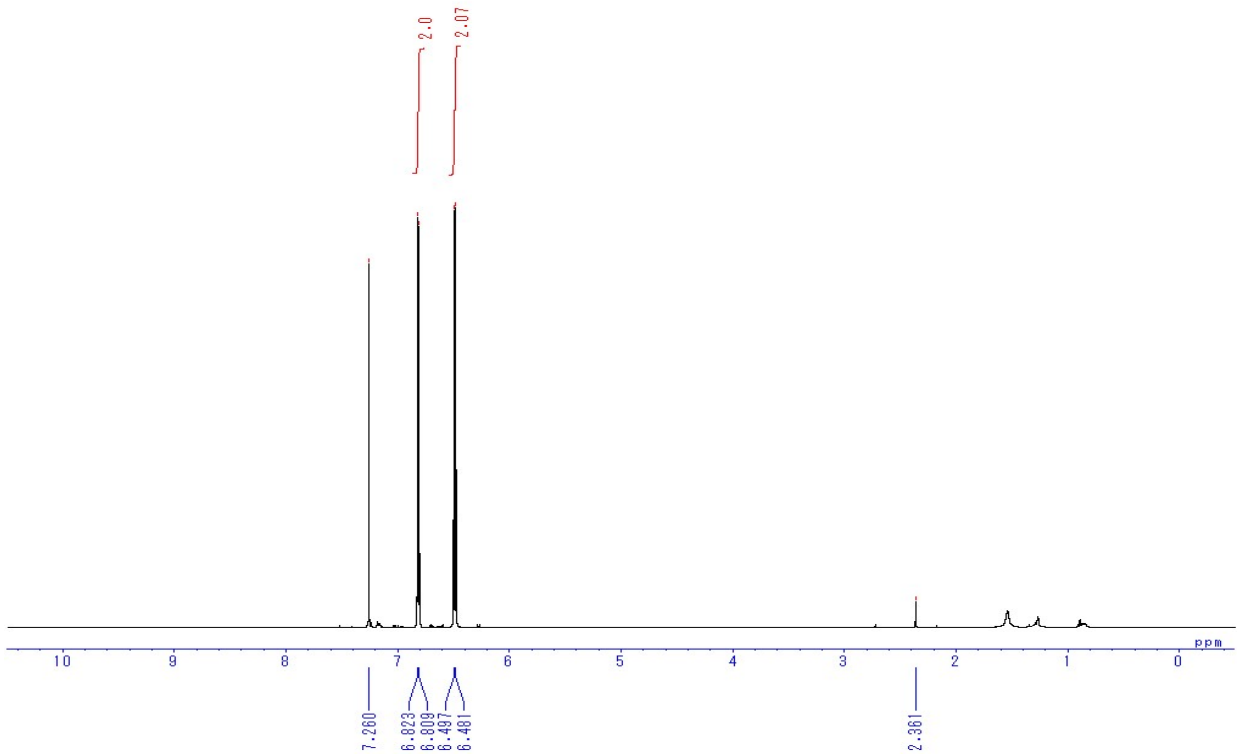

Fig. S15.23 ^{1}H NMR spectrum of **14**

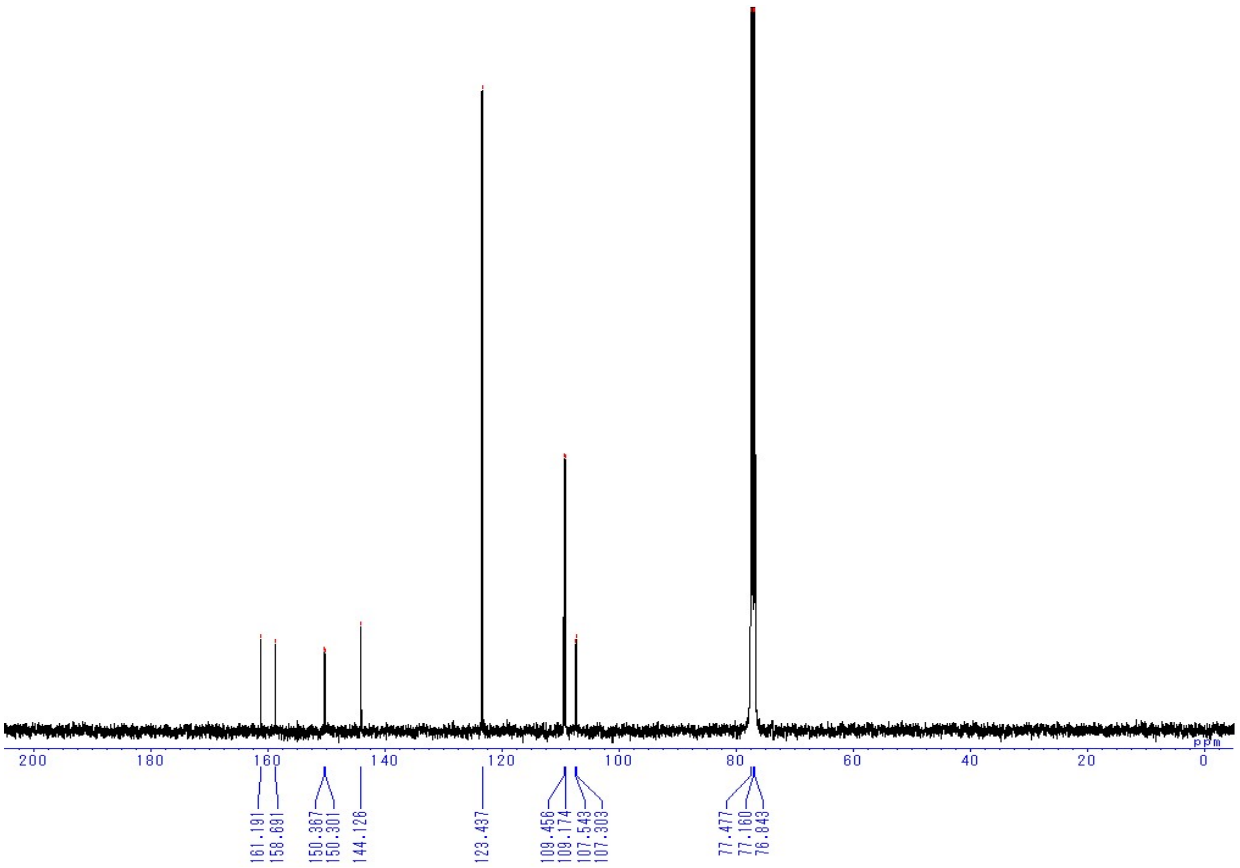

Fig. S15.24 ^{13}C NMR spectrum of **14**

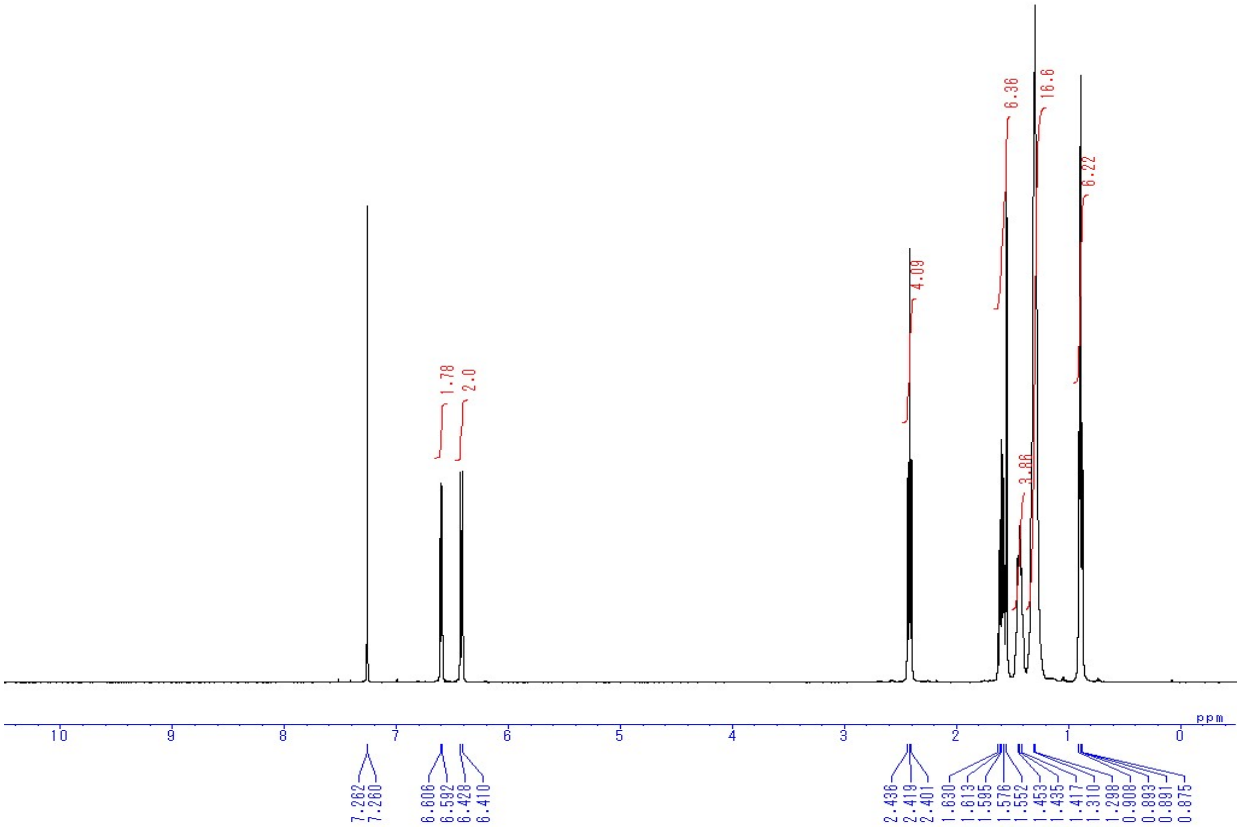

Fig. S15.25 ^{1}H NMR spectrum of **15**

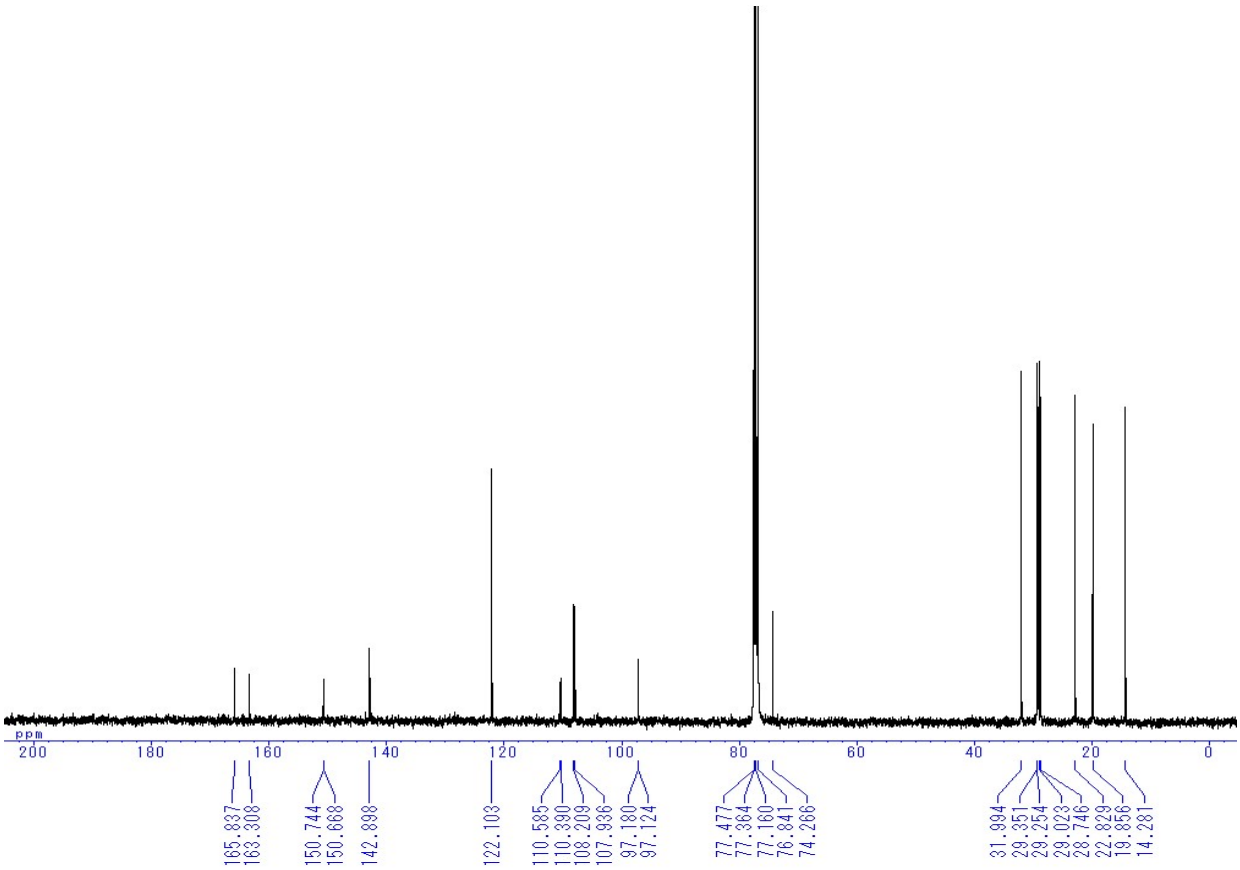

Fig. S15.26 ^{13}C NMR spectrum of **15**

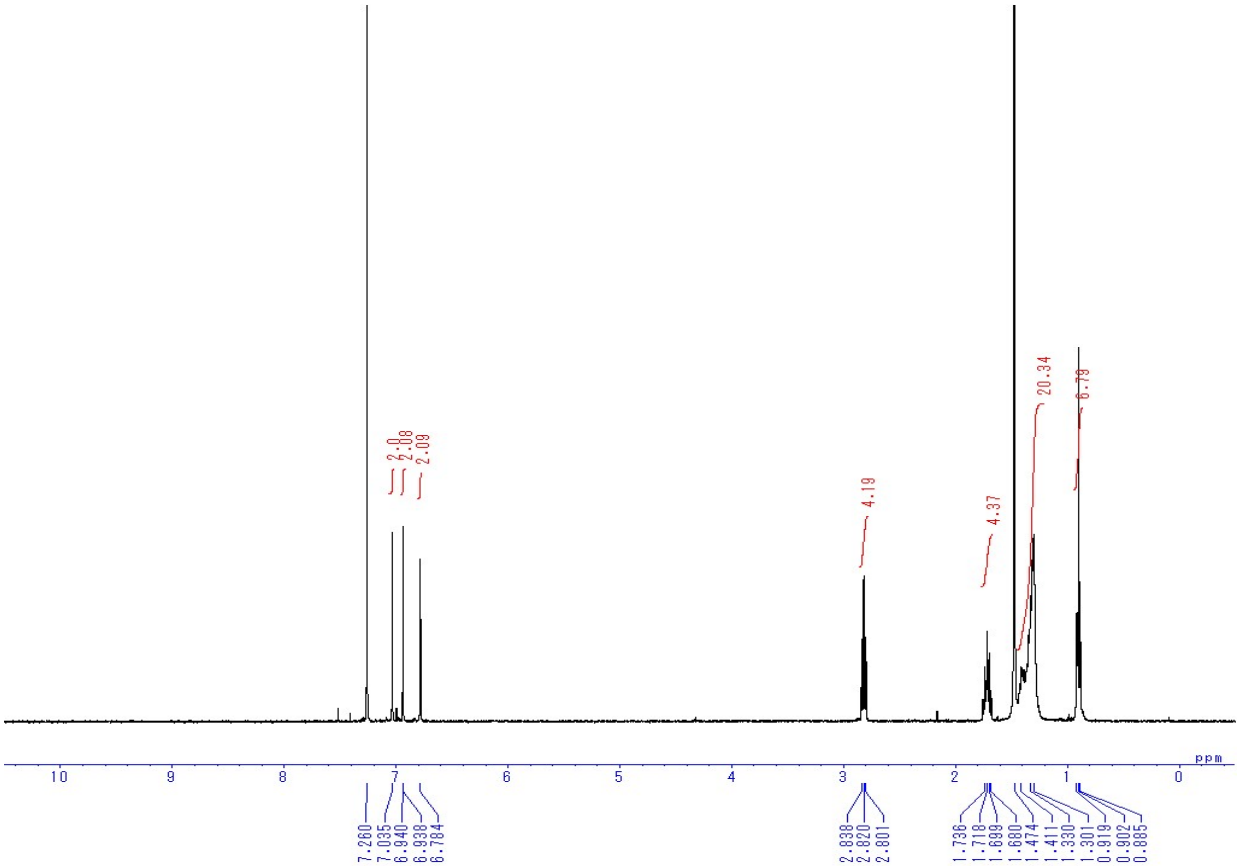

Fig. S15.27 ^{1}H NMR spectrum of **C8-L-BPDT**

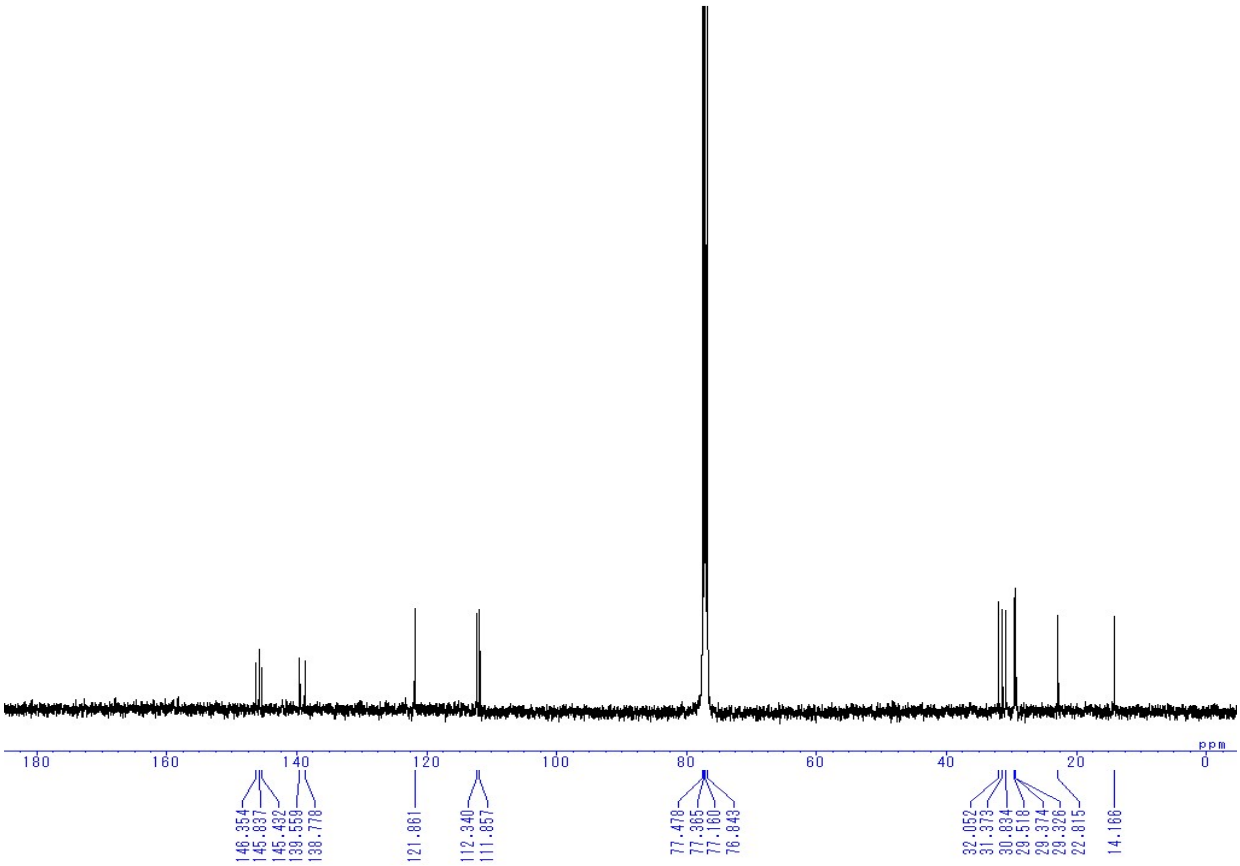

Fig. S15.28 ^{13}C NMR spectrum of **C8-L-BPDT**